

Phytoplankton community structure in the Kandla port ecosystem situated in a creek in the Gulf of Kutch, India

Aseem R. Rath^{1,2}, Smita Mitbavkar^{1*}, Arga Chandrashekar Anil¹

¹Council of Scientific and Industrial Research, National Institute of Oceanography,
Dona Paula, Goa 403 004, India

²School of Earth, Ocean, and Atmospheric Sciences, Goa University,
Taleigao Plateau - 403 206, Goa, India

*Corresponding author; email: mitbavkars@nio.org

Aseem R. Rath: aseemdolphin14@gmail.com

Arga Chandrashekar Anil: anilac@gmail.com

Abstract The port ecosystems are prone to deterioration due to the maritime and coastal activities and as a major source of the country's economy need efficient management. Phytoplankton communities can serve as reliable indicators of the prevailing environmental conditions due to their short life cycles. Seasonal sampling was conducted at 26 stations from October-2014 to February-2016 at Kandla port situated in a creek, along the west coast of India. The post-monsoon and monsoon water temperatures were higher (30°C) whereas pre-monsoon were lower (21°C). The salinity varied from polyhaline (18-30; monsoon) to euhaline (30 to 45; non-monsoon). The strong currents, high tidal activity, shallow depth areas, and the creek backwater systems make this ecosystem well-mixed and turbid. The annual average trophic index (TRIX) scores indicated very good water quality and low eutrophication, except during pre-monsoon (2.3 ± 0.7 to 4.1 ± 0.2). Based on the cell size, the phytoplankton community was classified into two main groups i.e., nanomicrophytoplankton, which comprised forty seven species (represented by diatoms, dinoflagellates, and silicoflagellates) and picophytoplankton including two groups (Picocyanophytes and picoeukaryotes). The diatoms and picophytoplankton dominated the total biomass and cell abundance, respectively. Only the picophytoplankton exhibited significant seasonal variations in cell abundance and carbon biomass. The lowest monsoon phytoplankton abundance coincided with high turbidity and vice versa during the post-monsoon. The hypersaline pre-monsoon environment with lower annual temperature, relatively lower turbid waters, and increased nutrients favoured higher diatom diversity. These conditions also supported potentially harmful *Gymnodinium* sp. and bloom-forming *Tripos furca* and *Pyrophacus* sp. Overall, ten non-toxic but bloom-forming species were observed. The study provides insights into the phytoplankton community's response to environmental conditions that can have repercussions on the ecosystem's functioning.

Keywords Diatoms, Hypersaline, Harmful algae, Dinoflagellates, Picophytoplankton; Turbidity

Introduction

The Indian peninsular coastline has several ports, which play an important role in the country's economic growth. These ecosystems are under a constant threat of pollution from the coastal industries, maritime activities, and inhabitants thereby influencing the ecosystem functioning and human health. The introduced pollutants could be of chemical (eg. inorganic nutrients, heavy metals) or biological (toxic, harmful microorganisms) nature depending on the source. In view of the importance of such ecosystems, appropriate measures need to be adopted for their efficient functioning. The most effective and reliable strategy to address the issue of aquatic ecosystem disturbance is to have baseline information on the phytoplankton community that can serve as a guide for future environmental monitoring and assessment. In addition, evaluation of the phytoplankton community in relation to the prevailing hydrographical and environmental parameters will give better insights into the phytoplankton ecology.

Phytoplankton are the foundation of aquatic food webs and modifications in its structure results in cascading effects on the food web. They serve as effective bioindicators of environmental health due to their short life cycles (Desrosiers et al., 2013). Therefore, the knowledge about factors that regulate phytoplankton community structure, abundance, and biomass is vital for understanding the functioning or restoration of any aquatic ecosystem (Mozetic et al., 2019; Soler-Figueroa et al., 2020). The phytoplankton community comprises microscopic photosynthetic organisms with cell sizes ranging from 0.6 to 200 μm . These organisms are grouped based on cell size into three categories viz. picophytoplankton (0.2 to 3 μm ; Pico), nanophytoplankton (> 3 to 20 μm), and microphytoplankton (> 20 to 200 μm). Most of the studies deal only with nano-microphytoplankton (NMP) due to technical or financial constraints. The inclusion of the Pico group can have additional benefits in understanding the responses of the entire phytoplankton community as cell size plays a vital role in the ecology and biogeochemistry of aquatic ecosystems. These small sized cells, which were neglected so far can also have a role to play in the ballast water intake and discharge at the ports (Soler-Figueroa et al., 2020).

Along with cell numbers, the carbon biomass estimations provide valuable insights into the phytoplankton group contribution to the total phytoplankton biomass (Snoeijs et al., 2002; Cornet-Barthaux et al., 2007). Phytoplankton carbon biomass is a basic parameter in ecosystem models as it influences the higher trophic level species richness and biomass. It also helps in the quantification and prediction of the exported primary production (Menden-Deuer & Lessard, 2000). Hence, phytoplankton biomass studies can help to understand the food web functioning at higher levels in coastal ecosystems.

The present study was carried out at the Kandla Port Trust (KPT), a major port located along the west coast of India in the Gulf of Kutch. The port is situated in the Kandla creek and is influenced by the coastal industries, salt pans, mangrove ecosystem, and the Arabian Sea. The port ecosystem experiences macrotides (maximum of ~ 6.6 m tidal range) and is highly turbid throughout the year (Babu et al., 2005). Literature survey shows that the studies on the phytoplankton community from this region are very scarce and preliminary (Ramamurthy & Dhawan, 1967; Dhawan, 1970). There are no in-depth investigations that deal with the inter-relationships between phytoplankton and the ambient environmental and hydrographical conditions. Hence this study will be a useful contribution towards the understanding of the ecosystem's phytoplankton community including the presence of any harmful or toxic species. The main aim of this study was to investigate the 1) seasonal and spatial variations in the NMP and Pico community structure, cell abundance and carbon biomass, 2) the relation of phytoplankton with the prevailing hydrographical and environmental conditions, and 3) the presence of toxic or harmful phytoplankton species.

Materials and Methods

Study area

The Kandla Port Trust or Deendayal Port Trust (Latitude 23° 01' N and Longitude 70° 13' E) is a seaport in the Kutch District of Gujarat state in western India. It is a natural harbor situated on the western side of the Kandla creek that meets the Gulf of Kutch (GoK) at a distance of 90 nautical miles from the Arabian Sea (Fig. 1). The GoK experiences a high tidal range (maximum of ~ 6.6 m at Kandla) and currents (Babu et al., 2005). The channel width varies from 200 m upstream to 1,000 m downstream. The Gulf extends on the eastern side into the little Rann of Kutch, a salt marsh (where salt panning is a seasonal activity) through numerous creeks whose bottom is muddy. The KPT is an all-weather port. Small creeks protected by mangroves on the eastern side are influenced by seawater intrusion from the Arabian Sea (Shirodkar et al., 2010). The western side is equipped with port activities, industries, and salt marshes. The strong currents (Sinha et al., 2006), high tidal activity, low depth areas (mangrove areas), and the creek backwater systems make this ecosystem well-mixed and turbid. The port ecosystem was categorized into three zones based on the location, 1) Industrial (stations 1 to 8; depth range: 7 to 13 m), 2) major Activity (stations 9 to 20; depth range: 7 to 20 m, increasing downstream) on the western side and 3) Mangrove (stations 21 to 26; depth range: 4 to 6 m with a minimum during the monsoon season) on the eastern side.

Sampling and sample analyses

The study region experiences three seasons i.e., monsoon (June to September; MON), post-monsoon (October to January; PoM), and pre-monsoon (February to May; PrM). The samplings were conducted on four occasions, which included two consecutive PoMs (October 2014 and November 2015; PoM-I and PoM-II, respectively), MON (July 2015), and PrM (February 2016). This study was a part of the project 'Ballast Water Management Program, India' involving creation of a port baseline data of eight major Indian ports. The sampling across three seasons and a repeat for one season was done (i) to check for variability within seasons and (ii) also as a project requirement. Altogether 26 stations were sampled from the surface and near bottom ($n = 26$ stations \times 2 depths \times 4 seasons = 208 samples; Table 1; Fig. 1). The surface and near-bottom water (NBW; ~ 1 m above the sea bottom) samples were collected with a Niskin sampler for environmental [salinity (100 mL), dissolved oxygen (DO; 125 mL), biological oxygen demand (BOD; 125 mL), suspended particulate matter (SPM), chlorophyll *a* (chl *a*; 250 mL), nutrients {nitrate (NO_3^-), nitrite (NO_2^-), ammonium (NH_4^+), phosphate (PO_4^{3-}) and silicate (SiO_4^{4-}); 4 mL each}], and biological [Pico (2 mL in duplicates and NMP (500 mL in duplicates)] parameters. The station-wise water temperature and depth were recorded *in situ* with a multiparameter Sonde DS5X (Hydrolab). The salinity and nutrient samples were stored in cool conditions for subsequent analysis. The samples for chlorophyll *a* analyses were filtered through 0.7 μm GF/F filters and stored at -20°C until analysis. The samples for Pico (1.8 mL in triplicates) analyses were preserved with paraformaldehyde (0.2% final concentration) and stored at -80°C in the laboratory until analysis. The NMP samples were preserved with Lugol's Iodine solution (1% final concentration) and stored at room temperature until analysis. The nutrients, DO, BOD, and chl *a* samples were analysed according to standard protocols (Parsons et al., 1984). A FlowCAM FCVS4 (Fluid Imaging Technologies, USA; D'Anjou et al., 2014; Rath et al., 2021) was used to measure the SPM. The rainfall and tide data were acquired from the Indian Meteorological Department (IMD).

Picophytoplankton analyses

After thawing to room temperature, internal standard (yellow-green latex beads of 2 μm ; Fluoresbrite® YG Microspheres - Polysciences Co., USA) to calibrate cell fluorescence emission and light scatter signals were added to the water samples. The analyses were carried out with a flow cytometer (BD FACSAria™ II) equipped with a blue (488 nm) and red (633 nm) laser, capable of detecting red fluorescence emitted by chlorophyll and phycocyanin pigments, respectively. After the analyses, the light scatters (cell size proxies) and fluorescence [red fluorescence from chlorophyll (> 650 nm), and phycocyanin (630 nm) pigments; orange fluorescence from phycoerythrin (578 nm)]

parameters were used to demarcate the Pico clusters on the dot plot and estimate the cell abundance (Mitbavkar et al., 2012). BD FACSDiva™ software was used for data processing.

Nano-microphytoplankton analysis

The supernatant from the undisturbed (48 h) NMP samples was siphoned out through a 10 µm mesh with the help of a silicon tubing to obtain 100 mL concentrated sample (Rath et al., 2018). The samples were subjected to qualitative and quantitative microscopic analysis and the taxonomic positions of the encountered NMP species were classified according to internationally accepted platform for recently accepted names (<http://www.algaebase.org/>, Subrahmanyam, 1946; Desikachary, 1987; Desikachary & Prema, 1987; Tomas, 1997; Horner 2002). The toxic/non-toxic categorization of the phytoplankton species was done based on the IOC-UNESCO taxonomic reference list of harmful microalgae (Moestrup et al., 2009). The phytoplankton group-based carbon biomass (pg C L⁻¹) was calculated from the species biovolume measurements (Menden-Deuer & Lessard, 2000; Worden et al., 2004).

Trophic status of KPT ecosystem

The multivariate index of trophic state (TRIX) method was used to estimate the trophic status of the KPT ecosystem (Vollenweider et al., 1998; Sin et al., 2013; Rath et al., 2018). The relationship between NMP and the trophic status of water was assessed using the TRIX scores. TRIX was calculated by the equation $TRIX = (\log_{10} (\text{chl } a \times \text{a\%O}_2 \times \text{DIN} \times \text{DIP}) + k)/m$, where chl *a* is in mg m⁻³, a%O₂ is the absolute value of the percentage of DO saturation ($\text{abs } |100 - \%O_2| = \%O_2$), DIN is dissolved inorganic nitrogen including NO₃⁻, NO₂⁻, and NH₄⁺ in mg m⁻³, and DIP is dissolved inorganic PO₄⁴⁻ in mg m⁻³. The constants k-3.5 and m-0.8 are scale values obtained from Vollenweider et al. (1998) to adjust TRIX scale values (reads from 0 to 10) with a level of eutrophication in the sampling area (TRIX score for water quality: < 4 = high state with low eutrophication; between 4 and 5 = good state; between 5 and 6 = bad state with high eutrophication; > 6 = very poor state with high eutrophication levels).

Data analyses

The seasonal, zonal, and depth-wise variations in the environmental variables, phytoplankton abundance, and biomass were examined through the Permutational Multivariate Analysis of Variance (PERMANOVA) using PRIMER v6 software with an add-on package PERMANOVA+. The relative contribution (%) of individual species to the total NMP abundance was estimated by using the mean values of surface and NBW data as significant depth-wise variations were not observed (Table 2). The seasonal and zonal distribution of the rare (contributing <1 % to the total NMP abundance) and

abundant (>1 % to the total NMP abundance) species were also assessed (Rodriguez-Ramos et al., 2014). The NMP surface and NBW abundance data were used to calculate the univariate measures (Shannon–Wiener diversity index: H' , Margalef's species richness index: d , and Pielou's evenness index: J') using PRIMER v.6 software. The similarity between the zones for each season with respect to the NMP abundance ($\log(x+1)$) was analysed using PRIMER v.6 software through the Bray-Curtis similarity and group-average method. The relationship between the environmental variables (temperature, salinity, DO, BOD, NO_3^- , NO_2^- , NH_4^+ , PO_4^{3-} , SiO_4^{4-} , and TRIX) and phytoplankton group's abundance as well as species abundance and sampling stations in the Industrial, major Activity and Mangrove areas of the KPT ecosystem was examined by employing the Redundancy Analysis (RDA). The analysis was selected through Detrended Correspondence Analysis (DCA). The forward selection and the Monte Carlo permutation test (999 unrestricted permutations) were used to determine the significant environmental variables explaining each group's/species' variation. CANACO 4.56 package (ter Braak & Smilauer, 2002) was used for performing the ordinations.

Results

Hydrography

The PerMANOVA analysis revealed significant variations in all the physico-chemical parameters with respect to seasons but not with zones and depths except salinity, DO, and NO_3^- that varied significantly with respect to seasons and zones (Table 2). The water temperature varied seasonally with highest values during the PoM-I (Surface: 30.1 ± 0.3 °C; NBW: 30.0 ± 0.3 °C) followed by MON (Surface: 28.1 ± 1.3 °C; NBW: 28.1 ± 1.2 °C) and PrM (Surface: 20.9 ± 0.1 °C; NBW: 20.8 ± 0.2 °C) (Fig. 2a, b; Supplementary Fig. 1a, b). The highest salinity was observed during the PrM (Surface: 39.8 ± 0.4 ; NBW: 38.8 ± 5.9) followed by the PoM-I (Surface: 37.7 ± 0.3 ; NBW: 37.8 ± 0.3) and the MON (Surface: 30.2 ± 10.2 ; NBW: 31.7 ± 8.7) (Fig. 2c, d; Supplementary Fig. 1c, d). The SPM load was higher during the MON (Industrial area: 46.2×10^3 ; major Activity area: 7.4×10^3 ; Mangrove area: 30.7×10^3 particles mL^{-1}) followed by PrM (Industrial area: 4.3×10^3 ; major Activity area: 10.3×10^3 ; Mangrove area: 1.8×10^3 particles mL^{-1}) with lower values during the PoM-I (Industrial area: 0.5×10^3 ; major Activity area: 3.7×10^3 ; Mangrove area: 2.8×10^3 particles mL^{-1}) and PoM-II (Industrial area: 5.4×10^3 ; major Activity area: 5.2×10^3 ; Mangrove area: 0.7×10^3 particles mL^{-1}). The surface DO concentrations ranged from 5.0 ± 0.4 (PoM-I) to 6.5 ± 0.6 mg L^{-1} (PoM-II) (Fig. 2e, f). The surface BOD values ranged from 2.2 ± 0.8 (PoM-II and MON) to 1.6 ± 0.8 mg L^{-1} (POM-I) (Fig. 2g, h). The chl *a* concentrations were higher during the PoM except in the Mangrove zone where MON showed higher concentrations (2i, j). The DIN concentrations peaked during the PoM-I as the NH_4^+ was significantly higher (15.3 ± 3.0 μM). The NO_3^- was highest

during PoM-II ($15.9 \pm 6.0 \mu\text{M}$) and lowest during PoM-I ($7.2 \pm 1.98 \mu\text{M}$). The NO_2^- was highest during MON ($7.0 \pm 1.8 \mu\text{M}$) and lowest during PoM-II ($3.0 \pm 0.5 \mu\text{M}$). The other nutrient concentrations were higher during the PrM (PO_4^{3-} : $5.3 \pm 0.8 \mu\text{M}$ and SiO_4^{4-} : $128.4 \pm 9.7 \mu\text{M}$) (Fig. 2k-t). The molar ratio of N:P exhibited a seasonal pattern with higher values during the PoM-II (5.49 ± 1.3 to 9.45 ± 2.3) and lowest during the PrM (3.9 ± 0.71 to 4.88 ± 0.9). The N:Si ratio remained low during all seasons (PoM: 0.43 ± 0.06 ; PrM: 0.18 ± 0.0 ; MON: 0.62 ± 0.18). The Si:P ratio was higher during PoM-II (24.2 ± 3.3 to 30.5 ± 4.8) and lower during MON (8.2 ± 1.8 to 10.6 ± 0.6). The chl *a* concentrations ranged from 0.3 ± 0.1 (PoM-II) to $1.1 \pm 0.5 \text{ mg m}^{-3}$ (MON) (Supplementary Table 1).

Phytoplankton community structure

The picophytoplankton ($< 3 \mu\text{m}$) and nano-microphytoplankton ($> 3 \mu\text{m}$) represented the phytoplankton community. Two groups represented the Pico community, picocyanophytes and picoeukaryotes. The NMP comprised 47 taxa representing three groups i.e., Bacillariophyceae (diatoms), Dinophyceae (dinoflagellates), and Dictyophyceae (silicoflagellates) (Table 3, Fig. 3a, b). The diatoms (41 species; 25 genera) were represented by centrics (16 species; 9 genera) and pennates (25 species; 16 genera). The dinoflagellates (4 species; 4 genera) were represented by phototrophic, heterotrophic, and mixotrophic types (2, 1, 1 species, respectively). The Dictyophyceae was represented by two species, *Dictyocha fibula* and *D. octonaria*.

Throughout the study period, the small-sized Pico dominated the total phytoplankton abundance while the relatively larger NMP dominated the carbon biomass (Fig. 4, 5). The Pico abundance (seasons and zones) varied significantly but not biomass (Fig. 4a, b; Fig. 5a, b; Table 2). During the PoM, the Pico abundance was higher (PoM II $>$ I) followed by PrM and least during the MON. A similar trend was observed in all three zones. The Pico biomass was higher during the PrM followed by PoM-II and MON and least during the PoM-I. The picocyanophytes dominated (65-74%) the Pico abundance during the PoM, which were taken over by the picoeukaryotes during PrM (97%) and MON (56%). The relative contribution of Pico to the total phytoplankton cell abundance ranged from 99.58 (MON) to 99.90 % (PoM-I).

The NMP did not exhibit significant seasonal variations (Table 2) in cell abundance [Surface waters: 7.4×10^3 (MON) to 26.2×10^3 (PoM-I) cells L^{-1} ; NBW: 5.7×10^3 (PoM-I) to 16.6×10^3 (PoM-II) cells L^{-1}] (Fig. 4c, d) and carbon biomass [Surface waters: 21.8×10^5 (PoM-I) to 88.5×10^5 (PrM) pg C L^{-1} ; NBW: 17.0×10^5 (PoM-I) to 64.6×10^5 pg C L^{-1} (MON)] (Fig. 5c, d). The diatoms dominated the NMP community in terms of numbers (Industrial area: 99.62 to 100%; major Activity

area: 99.66 to 100%; Mangrove area: 99.54 to 100%) and carbon biomass (Industrial area: 99.21 to 100%; major Activity area: 98.51 to 100%; Mangrove area: 99.41 to 100%) (Fig. 4e-j; 5e-j; 6a-h). In the surface waters, pennate diatoms dominated during PoM-I, PoM-II and PrM (Industrial area), MON (Mangrove area), and centrics during PrM and PoM-II (major Activity area), PoM-I (Industrial area) and MON (Mangrove area). During the PoM-I, pennate diatom *Fragilariopsis* sp. (15.4×10^3 cells L⁻¹) and centric diatom *Coscinodiscus radiatus* (2.4×10^3 cells L⁻¹) dominated the community in the Industrial area (Fig. 3a; Table 4). During PrM, pennate diatoms *Fragilariopsis* sp. (Industrial area: 14.5×10^3 cells L⁻¹), *Thalassiothrix longissima* (major Activity area: 6.8×10^3 cells L⁻¹), and centric diatom *Thalassiosira* sp.1 (major Activity area: 9.6×10^3 cells L⁻¹) dominated the community. During PoM-II, pennate diatom *Fragilariopsis* sp. (Industrial area: 13.9×10^3 cells L⁻¹) and centric species *Thalassiosira* sp.2 (Industrial area: 8.3×10^3 cells L⁻¹), *Paralia sulcata* (major Activity area: 6.4×10^3 cells L⁻¹) were the dominant forms in the diatom community. The MON community was dominated by the centric diatom, *Thalassiosira* sp.2 (major Activity area: 9.1×10^3 cells L⁻¹) and pennate diatom, *Nitzschia* sp.1 (higher in the Industrial and Mangrove area).

The dinoflagellate abundance and biomass were higher in the major Activity area (Fig. 4k-r; Fig. 5k-r). The highest numbers were observed during the PrM [0.08×10^3 cells L⁻¹ (0.34 %)] followed by PoM-II [0.04×10^3 cells L⁻¹ (0.24 %)]. The carbon biomass was highest during the PrM [1.1×10^5 pg C L⁻¹ (1.28%)] followed by MON-II [0.34×10^5 pg C L⁻¹ (0.79%)]. *Pyrophacus* sp. and *Tripes furca* were the dominant species during the MON and PrM, respectively. During the PoM-I, *Protoperdinium* sp. and *T. furca* were the dominant species.

The silicoflagellates were the least abundant group with the highest abundance (0.004×10^3 cells L⁻¹; 0.2%) and biomass (0.96×10^5 pg C L⁻¹; 2.2%) in the surface waters of the Industrial area during the PoM-I (Fig. 4s,t; 5s, t). *Dictyocha octonaria* was higher in numbers during PoM-I and *Dictyocha fibula* during the MON, PoM-II, and PrM.

The overall similarity between zones with respect to the surface NMP community abundance was > 50%. The similarity values for the surface community ranged between 60 to 80% for MON and PrM, 80% for POM-II and 65-80% for POM-I. In case of the NBW community, the similarity for PoM-I ranged from 75 to 85%, PrM from 80 to 65%, PoM-II from 80 to 85%, and MON from 75 to 80%. The MON season was the most dissimilar season with respect to the surface NMP abundance. With respect to zones, the Industrial zone was least similar (50-60%) during the MON and POM-I whereas during the POM-II and PrM, the Mangrove zone was the least similar (~ 60%). In the NBW, the POM-I was the most dissimilar season (~ 60%). The Mangrove zone was least similar during

POM-I and POM-II (75-80%). During MON and PrM, the major activity zone was least similar (Suppl. Fig. 2a, b).

Potential harmful species

The pennate diatom, *Pseudo-nitzschia* sp., and phototrophic dinoflagellate *Gymnodinium* sp. were the two toxic and potentially harmful species observed in the NMP community. *Pseudo-nitzschia* sp. and *Gymnodinium* sp. were abundant only during PrM in the Mangrove (0.70×10^3 cells L⁻¹) and Industrial (0.14×10^3 cells L⁻¹) areas, respectively (Fig. 3b). Additionally, ten non-toxic but bloom-forming species were observed during the study period. *Coscinodiscus radiatus*, *Ditylum brightwellii*, *Rhizosolenia imbricata*, *Thalassiosira* spp., *Triceratium favus*, *Fragilariopsis* sp., *Thalassionema nitzschioides*, *T. longissima*, *Protoperidinium* sp., *T. furca*, and *D. fibula* were the bloom-forming species. *C. radiatus*, *Fragilariopsis* sp., *T. longissima* were the dominant species with higher abundance during the non-monsoon seasons whereas *Thalassiosira* spp. during MON season (Table 4).

TRIX scores and diversity index

The TRIX scores ranged between 3.1 (Mangrove area) and 4.1 (Industrial area) during the PrM in the surface waters whereas, in the NBW, it ranged between 2.3 (in the Industrial area during MON) and 3.8 (in the Industrial area during PrM) (Table 5). The scores indicate a high state of water quality and low eutrophication, except during the PrM (Industrial area), where a good state of water quality was observed.

The NMP H' was highest in the surface waters (2.07; Mangrove area) during PrM and lowest in the NBW (1.27; major Activity area) during PoM-I (Table 5). The NMP d was highest (1.36; Industrial area) during PrM in the surface waters and lowest (0.56; major Activity area) during PoM-I in the NBW. The J' values ranged between 0.72 (PoM-I; Mangrove area; surface waters) and 0.84 (PoM-I; Industrial area; NBW) depicting an evenly distributed community throughout the study period, except during the PoM-I.

Relative contribution of nano-microphytoplankton groups

The relative contribution of centric diatoms was comparatively lower than pennates in abundance whereas higher in terms of biomass during every season except MON. The dinoflagellates were higher in contribution during PrM followed by MON abundance wise whereas in terms of biomass it was higher during PoM-I followed by PrM. The silicoflagellates were higher during PoM-I in terms of abundance and biomass.

Relation between phytoplankton and environmental factors

NMP group's: In the Industrial area, the first and second RDA axes explained 19% of the variability in phytoplankton group's abundance and 87.4% of the relationship between the abundance and environmental factors (Fig. 7a, Table 6). Temperature, salinity, NH_4^+ and SiO_4^{4-} were the significant factors ($p \leq 0.05$). The Dinophytes correlated negatively with temperature. SiO_4^{4-} concentrations positively influenced the Bacillariophytes and Dictyophytes. The Pico correlated positively with temperature, salinity, and NH_4^+ .

In the major Activity area, the first and second RDA axes explained 20.2% of the variability in phytoplankton groups' abundance and 97.8% of the relationship between the abundance and environmental factors (Fig. 7b, Table 6). NO_3^- , NO_2^- , and SiO_4^{4-} were the significant factors ($p \leq 0.05$). The Bacillariophyceae, Dinophyceae and Dictyophyceae correlated negatively with temperature and positively with SiO_4^{4-} and NO_3^- . The Pico correlated positively with temperature and NH_4^+ .

In the Mangrove area, the first and second RDA axes explained 15% of the variability in phytoplankton group's abundance and 86.7% of the relationship between the abundance and environmental factors (Fig. 7c, Table 6). NO_2^- and SiO_4^{4-} were the significant factors ($p \leq 0.05$). The Bacillariophyceae, Dinophyceae, and Dictyophyceae correlated negatively with NO_2^- . The Pico correlated positively with salinity and nutrients.

NMP species: In the Industrial area, the NMP species were significantly ($p \leq 0.05$) influenced by NH_4^+ , SiO_4^{4-} , PO_4^{3-} , salinity and temperature (Table 7). The 25.2% of the variability in the abundance and 67.6% of the relationship between abundance and the environmental variables was explained by the first two RDA axes (Fig. 8a). The temperature strongly related to axis 1 and salinity to axis 2 (Fig. 8a, b). The environmental variables explained 39.3% of the total inertia (1.0). The RDA axis 1 and 2 (eigenvalues of 0.15 and 0.11, respectively) explained 67.6% of the cumulative variance of the relationship between species and environmental variables. During PoM-I and PrM, the Bacillariophyceae correlated positively with the nutrients and salinity. They also exhibited a negative correlation with temperature during the PrM and a positive correlation during the PoM. *C. radiatus* correlated positively with NH_4^+ (PoM-I), *T. longissima* with PO_4^{3-} (PoM-I, PrM), and *Fragilariopsis* sp. with salinity (PoM-I, PrM). The Dinophytes correlated negatively with the temperature.

In the major Activity zone, the temperature, NH_4^+ , SiO_4^{4-} , and salinity significantly ($p \leq 0.05$) influenced the NMP species (Table 7). The first two RDA axes explained 26.2% of the variability in

the abundance and 78% of the relationship between abundance and the environmental variables (Fig. 8c, d). The temperature strongly related to axis 1 and salinity to axis 2. The environmental variables explained 53.9% of the total inertia (1.0). The RDA axis 1 and 2 (eigenvalue of 0.181 and 0.081, respectively) explained 78% of the cumulative variance of the relationship between species and environmental variables. A positive correlation was observed between the Bacillariophyceae salinity and nutrient concentrations (PrM: NO_3^- , NO_2^- , PO_4^{3-} , SiO_4^{4-} and PoM-I: NH_4^+). *T. longissima*, *Thalassiosira* sp.1, and *P. sulcata* positively correlated with SiO_4^{4-} and negatively with temperature during PrM. *C. radiatus* (POM-I) correlated positively with NH_4^+ . *Fragilariopsis* sp. was observed during PoM and PrM indicating that temperature is not a controlling factor and was positively correlated with SiO_4^{4-} . The Dinophytes positively correlated with NO_3^- , NO_2^- and SiO_4^{4-} .

In the Mangrove area, the temperature, NH_4^+ , SiO_4^{4-} , and NO_2^- significantly ($p \leq 0.05$) influenced the NMP species (Table 7). The first two RDA axes explained 29% of the variability in the abundance and 70.5% of the relationship between abundance and the environmental variables (Fig. 8e, f). The temperature correlated to axis 1 and NO_2^- to axis 2. The environmental variables explained 46.4% of the total inertia (1.0). The RDA axis 1 and 2 (eigenvalue of 0.19 and 0.10, respectively) explained 70.5% of the cumulative variance of the relationship between species and environmental variables. The Bacillariophyceae correlated positively with NO_3^- and negatively with temperature, salinity, and nutrients. *C. radiatus* (POM-I) correlated positively with NH_4^+ . *Fragilariopsis* sp. exhibited a positive correlation with SiO_4^{4-} and salinity. *T. longissima* correlated positively with SiO_4^{4-} .

Discussion

Variability in hydrological and environmental parameters

The vertical distribution of water temperature and salinity throughout the study period indicated a well-mixed water column in the KPT ecosystem. The macrotidal nature of this region combined with shallow depth areas and creek backwater systems generate highly turbid waters (Sinha et al., 2006). The Kandla port ecosystem experiences a marine to hypersaline environment throughout the year. The low salinity in the Industrial and Mangrove zones in July 2015 (MON) could be attributed to the lower tidal height and freshwater discharge from the rivers Bana, Saraswati, and Machhu, which establish a connection with the Gulf on its inner side through the little Rann of Kutch during the south-west monsoon (Shirodkar et al., 2010). The high saline waters in the major Activity zone indicate a lack of river water influence and seepage of brine from the ambient salt pans through monsoonal drainage. The high saline waters during the non-monsoon seasons, especially the PrM is

due to the dissolved salts brought into the creek by the tributaries and the evaporation of water in the creek caused by the arid climate (Shirodkar et al., 2010).

Phytoplankton community response to environmental conditions

The investigations on plankton ecology are very scarce from the KPT ecosystem. The phytoplankton community structure varied due to the seasonal hydrography and physico-chemical environmental conditions. The dominance of the phytoplankton community by the Pico in terms of cell numbers was similar to that reported in the other coastal regions of India (Rath et al., 2021). The highest Pico abundance during the PoM coincided with the highest seasonal temperature, high nutrient concentrations, and lower SPM, signifying the importance of higher light availability. The lower abundance during the MON despite the higher water temperature could be attributed to the higher turbidity-induced lower light availability. Likewise, during the PrM, the lower temperatures could have led to the lower abundance of Pico although the light availability was high. These observations indicate a synergistic role of temperature and light in influencing the seasonal distribution of the Pico community. Although small, as this group includes some toxic forms, the high abundance, with > 90% contribution to the total phytoplankton community abundance can have implications in the ballast water management protocols in the port ecosystems, which at present include only the > 10 μm to < 50 μm cell size range (Soler-Figueroa et al., 2020). However, this group was not dominant in terms of carbon biomass due to their smaller cell size as compared to the NMP. The NMP group was dominated by diatoms in terms of cell abundance and carbon biomass, which could be attributed to the turbulent environment (Margalef, 1978). The diatoms also dominated the total phytoplankton biomass due to their large cell size and rapid growth supported by their intensive uptake of nutrients (*r*-strategists). On the contrary, the turbulent waters with low light availability could have negatively influenced the dinoflagellates and silicoflagellates growth, which usually have slower growth rates (*K*-strategists) than diatoms and prefer stable environments (Spilling et al., 2014; Smayda & Reynolds, 2001). However, the diatoms in the KPT ecosystem were relatively lower in numbers compared to the less turbid tropical coastal regions (Patil & Anil, 2011; Rath et al., 2018; Rath et al., 2021). This observation was substantiated by earlier studies in the Gulf of Kutch (Dhawan, 1970). The low concentrations may be attributed to the turbid nature of the water column due to the macrotides (maximum tidal elevation of 6.6 m; Babu et al., 2005). This could have resulted in an insignificant seasonal and zonal variation in the NMP abundance and biomass in the surface and NBW (Table 2; Suppl. Fig. 2a, b). However, in case of Pico the effect of water temperature and salinity overrides that of irradiance (Mitbavkar et al. 2012), which could have significantly affected the cell abundance with respect to seasons and zones, respectively, but not depth. The light

penetration into the water column also gets affected due to the high turbidity throughout the year. Dhawan (1970) reported Secchi disc depth of not more than half a meter during most of the year and as low as 15 cm during the southwest monsoon. This could have led to the significant variation between the surface and near bottom NMP abundance.

The seasonal peak in NMP abundance and carbon biomass observed during the warmer PoM-I, suggests the proliferation of eurythermal species or those adapted to warm temperatures. The reduced nutrient concentrations (NO_3^- , SiO_4^-) and higher chl *a* biomass further substantiates the high photosynthetic rates that could have been accentuated by the better light availability due to the lowered turbidity. Similar conclusions were drawn from a previous investigation in the present study region, which reported high productivity (Shirodkar et al., 2010). Another probable reason for the peak in NMP abundance and carbon biomass could be the coinciding high concentrations of NH_4^+ introduced into the port waters by the spillage from chemical manufacturing industries during the loading or unloading processes. The diatoms and silicoflagellates showed a positive correlation with salinity and NH_4^+ . Both, culture and field experiments have demonstrated a preference for uptake and assimilation of NH_4^+ over other inorganic nitrogen concentrations by diatoms but this process is species-specific and depends on some environmental factors such as temperature and light intensity (Lomas & Glibert, 1999a, b; Glibert et al., 2016). The higher NMP abundance and carbon biomass dominated by diatoms, and lower diversity, richness, and evenness were due to the dominance of a few diatom species such as *T. longissima*, *C. radiatus*, *Fragilariopsis* sp., and *Diploneis* sp. The dominance of these species during other seasons also indicates a eurythermal nature except *C. radiatus*, which could be a warm temperature adapted species. Amongst the zones, the relatively higher NMP abundance and carbon biomass in the Industrial Area (Suppl. Fig. 2a) and the positive correlation of *C. radiatus* with temperature and NH_4^+ only during the PoM-I could indicate interactive effects of the two environmental factors on the diatom growth rates. The NO_3^- concentrations, and warming had significant interactive effects on promoting specific growth rates, cellular chl *a* content, and N:P ratio of *Coscinodiscus* sp. (Qu et al., 2018). *Thalassiosira pseudonana*, *T. weissflogii* and *Cyclotella cryptica* under high concentrations of NH_4^+ exhibited key sexual morphologies such as oogonia, spermatogonia and auxospores, with the onset of the stationary phase (Moore et al., 2017). The lowered nutrient concentration led to a reduced NBW community in the Mangrove area during the PoM season (Suppl. Fig. 2b).

According to earlier literature from the study site, the summer blooms peak during September (Dhawan, 1970). As our sampling was conducted in October and November, the observed relatively smaller NMP peaks could be the waning phase of the bloom that would have initiated in September.

The cell abundance decline was also reflected in the chl *a* concentrations of the two PoM sampling periods. Thus sampling in the PoM season at different intervals after the end of MON season gives an idea about the phytoplankton response during the immediate transition phase and thereafter. A spill-over of the monsoon effect can be expected in the first PoM sampling (October) when the environmental conditions such as nutrient concentrations are favourable followed by a gradual decline in the NMP due to the consumption of nitrate and silicate (November). These responses of the NMP could have been masked if the two sampling data were combined. The observed variabilities also indicate that future studies have to incorporate high frequency intra-seasonal samplings to have a thorough understanding of the phytoplankton community dynamics. The diatom bloom collapse and the genetic diversity that seeds future blooms may be controlled by the sexuality induction (Moore et al., 2017). The presence of *Coscinodiscus* sp. in lower numbers during the other seasons could indicate the formation of resting spores that sink to the bottom sediment to form a viable ‘seed bank’, which gets re-suspended and rejuvenated serving as an inoculum during the favorable conditions (McQuoid, 2005; Hoppenrath et al., 2007; Patil & Anil, 2008). Similar observations were also made from the east coast of India (Rath et al., 2021).

Previous studies have shown that predators avoid microphytoplankton species, which form colonies, have external projections, and secrete mucilage (Sournia, 1982). A larger surface area also helps chain-forming diatoms to get maximum solar energy for photosynthesis, especially in turbid waters (Finkel et al., 2010). The reducing tidal effect upstream along with the relatively shallower depth of the Industrial zone could be another contributing factor to the higher NMP in terms of the light availability and time spent in the euphotic zone. Shirodkar et al., (2010) reported spatial variability in the tidal factor, with higher values near the mouth and a decline towards the major Activity zone. Also, lower silicate concentrations and turbid waters favoured these long chain-forming diatom species (Dell’Aquila et al., 2017). *Protoperidinium* sp. and *D. octanaria* were the two species observed only during PoM-I in the Industrial area. The occurrence of heterotrophic (*Protoperidinium* sp.) and mixotrophic (*T. furca*) dinoflagellates during this season was corroborated by the positive correlation with temperature.

The lowest NMP abundance and carbon biomass during MON could be explained by the highly turbid water column caused due to the flooding of the Little Rann. The inundated vast mudflats bring enormous amounts of water rich in soft clays to the Kandla creek thereby affecting the underwater light availability for the NMP. A Secchi disc depth as low as 15 cm was reported during the southwest monsoon (Dhawan, 1970). The riverine influx from the adjacent rivers results in low saline waters in the Industrial and Mangrove areas. In contrast, the relatively higher salinity in the

major Activity area could be attributed to the influx of brine from the nearby salt pans through the tributaries of the creek and also land drainage as reported earlier (Shirodkar et al., 2010). The comparatively higher turbidity at the Industrial zone could have resulted in the lowest cell abundance thereby depicting lower similarity level with the other two zones (Suppl Fig. 2). The dominance of *Nitzschia* sp.1 in the Industrial and Mangrove zones where the salinity was ~ 20, indicates its introduction into the port ecosystem from the upstream brackish waters. This species along with *Thalassiosira* sp.2, and *Fragilariopsis* sp. which were dominant throughout the study area signify possession of survival adaptations such as high surface to volume ratios that help in maximizing access to ambient light and nutrients in highly turbid conditions (Finkel et al., 2010; Guinder et al., 2012).

During the PrM, the lower water temperature, relatively reduced water turbidity, and higher nutrient concentrations could have resulted in the NMP abundance and carbon biomass maxima. The highest species diversity and richness in the Industrial area also supports the view of a favorable environment during the PrM. Since this is a relatively calmer period of the year, without any influence from land drainage or precipitation, the fertilizer industries located in the Industrial area could be the source of the high nutrient concentrations, which later dissipate into the entire Kandla creek. *Fragilariopsis* sp., *Thalassiosira* sp.1, and *T. longissima* were the dominant diatom species in moderate abundance. Along with these, many other species were also abundant, which were suppressed during other seasons. *Coscinodiscus* sp., *Planktoniella blanda*, *Nitzschia* sp. 4, and *Pseudonitzschia* sp. along with the phototrophic dinoflagellate *Gymnodinium* sp. were observed only during PrM, which explains preferences towards higher nutrient concentrations, lower water temperatures, and high saline conditions. The comparatively lower cell abundance at the Mangrove area could be attributed to the lower nutrient concentrations and hence the lower similarity level with the other zones (Suppl. Fig. 2)

The bimodal phytoplankton abundance and carbon biomass maxima observed in the present seasonal study were similar to that reported earlier in this study region (Ramamurthy & Dhawan, 1967; Dhawan, 1970). The primary phytoplankton abundance and carbon biomass maxima coincided with the north-east monsoon (February) and the secondary with the post-south-west monsoon (October). According to Dhawan (1970), the phytoplankton abundance maxima during the northeast monsoon is a regular phenomenon supported by the lower temperature and high salinity. Since the fluctuation in the phytoplankton count was not reflected in the total plankton biomass volume, Dhawan (1970) attributed it to the zooplankton content. The phytoplankton biomass could be subjected to grazing pressure from copepods and planktonic larvae after the peaks. Dhawan (1970)

observed two peaks of copepods from March to September, which usually followed the phytoplankton maxima. The bi-modal seasonal phytoplankton peaks could be influencing the fisheries wherein a difference in the composition of prawns was reported in the GoK during August-September and October-November (Deshmukh, 1975).

The trophic status and occurrence of harmful algal species

The annual average TRIX score was 3.5 indicating very good water quality and low eutrophication, which could be attributed to the dilution effects caused by the vertically and horizontally well-mixed water column as a result of strong currents and macrotidal effects. Shirodkar et al., (2010) also concluded that the strong ebb tidal currents transfer the contaminants and sediment load from Kandla creek to the inner GoK. However, the highest TRIX score during the PrM (4.1) in the Industrial area, indicates that the port water quality may vary seasonally and regionally depending on the hydrography. Fertilizer-manufacturing industries such as IFFCO, salt industries, oil, and chemical manufacturing industries transactions and handling of liquid ammonia, POL, fertilizers, and industrial chemicals can make the Industrial area vulnerable to contamination (Shirodkar et al., 2010). The residence time was found to increase from the mouth to the head region of the GoK, with higher values during the PrM (Patgaonkar et al., 2012). The relatively calmer water circulation during this season could have resulted in poor water quality due to reduced flushing.

This is the first study that reported the seasonal distribution of harmful algal species in the KPT ecosystem. The toxic *Gymnodinium* sp. and bloom-forming *T. furca* and *Pyrophacus* sp. observed in the present study were previously reported from the Arabian Sea (Thangaraja et al., 2007; Al-Shehhi et al., 2014; Khokhar et al., 2018; Thomas et al., 2020). Their high abundance during the PrM could be because of the optimum nutrient availability and less turbid waters in the Mangrove area. The lower abundance of these species does not make this region vulnerable, but future changes in environmental conditions can trigger the occurrence of harmful algal blooms that could negatively influence the ecosystem. The toxic diatom *Pseudo-nitzschia* spp. produces domoic acid that leads to amnesic shellfish poisoning, creating gastrointestinal and neurological disorders that were reported in the coastal waters of the northeastern Arabian Sea (Thomas et al., 2020). *Pseudo-nitzschia* sp. were reported in high numbers from the southeastern coast of the Arabian Sea in the MON and PoM seasons (Padmakumar et al., 2012; Rath et al., 2018).

Conclusions

The KPT ecosystem exhibited a very good water quality with low eutrophication due to the well-flushed waters with low residence time brought about by the strong currents and macrotidal effects

during most of the year. However, the resultant high turbidity was reflected in the relatively lower phytoplankton abundance and biomass as compared to the other less turbid coastal waters. The community could represent the low-light adapted forms. The seasonal bimodal NMP abundance and carbon biomass peaks with varied species diversity and evenness in contrasting thermal ambiance (PrM and PoM) could have cascading effects on the higher members of the food chain and ultimately the fisheries. The unimodal peak of the Pico community during the PoM warm temperatures highlights the active microbial loop and its contribution to the classical food web. As the Pico community is known to include certain toxic forms, the > 90% contribution of the Pico to the total phytoplankton community abundance signifies the inclusion of this size group in the ballast water management regulations, which at present includes only the >10 µm to <50 µm cell size range. The high TRIX values during the PrM at the inner stations of the creek suggest seasonal variations in the flushing rate. This along with the presence of harmful/toxic dinoflagellates and diatoms, although with no reports of blooms/toxic effects, warrants regular ecosystem monitoring.

Acknowledgments

We thank The Director, National Institute of Oceanography (CSIR), for his support. We thank Dr. S.S. Sawant, Dr. D. V. Desai, and Mr. Venkat K. for their support and guidance. We thank the other project team members for their help during sampling. We gratefully acknowledge the project assistants (BAMPI) for the analysis of physico-chemical parameters. The authors thank the anonymous reviewers for their constructive comments. This work was supported by the Ballast Water Management Programme India, funded by Directorate General of Shipping, Government of India. This is a NIO contribution (no. #).

Author contributions

The study conception and design was done by A. C. Anil. The sampling, data collection and data processing was done by A. R. Rath. Data interpretation and manuscript writing was done by A. R. Rath and S. Mitbavkar. All authors approved the final version of the manuscript.

Funding

This work was supported by the Ballast Water Management Programme India, funded by Directorate General of Shipping, Government of India.

Data availability

The data obtained from this study appear in the submitted article and are available.

Competing interests

The authors declare no competing interests.

Declarations

All authors have read, understood, and have complied as applicable with the statement on "Ethical responsibilities of Authors" as found in the Instructions for Authors and are aware that with minor exceptions, no changes can be made to authorship once the paper is submitted."

References

- Al-Shehhi, M. R., Gherboudj, I., & Ghedira, H. (2014). An overview of historical harmful algae blooms outbreaks in the Arabian Seas. *Marine Pollution Bulletin*, 86, 314–24.
- Anderson, D. M., Sullivan, J. J., & Reguera, B. (1989). Paralytic shellfish poisoning in Northwest Spain: The toxicity of *Gymnodinium catenatum*. *Toxicon*, 27, 665-674.
- Babu, M. T., Vethamony, P., & Desa, E. (2005). Modeling tide-driven currents and residual eddies in the Gulf of Kachchh and their seasonal variability: a marine environmental planning perspective. *Ecological Modeling*, 184, 299-312.
- Cornet-Barthaux, V., Armand, L., & Queguiner, B. (2007). Biovolume and biomass estimates of key diatoms in the Southern Ocean. *Aquatic Microbial Ecology*, 48, 295-308.
- D'Anjou, R. M., Balascio, N. L. & Bradley, R. S. (2014). Locating cryptotephra in lake sediments using fluid imaging technology. *Journal of Paleolimnology*, 52, 257-264.
- Dell'Aquila G, Ferrante MI, Gherardi M, Lagomarsino MC, d'Alcalà MR, Ludicone D, & Amato A (2017). Nutrient consumption and chain tuning in diatoms exposed to storm-like turbulence. *Scientific Reports*, 7, 1828.
- Deshmukh, V.M. (1975). A note on the prawn fishery in the Gulf of Kutch during 1962-63. *Indian Journal of Fisheries*, 22, 265-269.
- Desikachary, T. (1987). Atlas of diatoms Fascicle 4: marine diatoms from the Arabian Sea and Indian Ocean. Madras Science Foundation.
- Desikachary, T., & Prema, P. (1987). Atlas of diatoms (diatoms from the Bay of Bengal), Madras Science Foundation, Madras. Fascicle-III.
- Desrosiers C., Leflaive, J., Eulin, A., & Ten-Hage, L. (2013). Bioindicators in marine waters: Benthic diatoms as a tool to assess water quality from eutrophic to oligotrophic coastal ecosystems. *Ecological Indicators*, 32, 25-34.
- Dhawan, R. M. (1970). Plankton and hydrological factors at Kandla in the Gulf of Kutch during 1960-1963. *Indian Journal of Fisheries*, 17, 122-131.
- Doan-Nhu, H., & Nguyen-Ngoc, L. (2017). Unusual fish killing blooms of *Tripos furca* in Van Phong Bay, South Viet Nam. *Harmful Algae News*, 57, 1–3.

- D'Silva, M. S., Anil, A. C., Naik, R. K., & D'Costa, P. M. (2012). Algal blooms: a perspective from the coasts of India. *Natural Hazards*, 63, 1225–1253.
- Finkel, Z. V., Beardall, J., Flynn, K. J. et al. (2010). Phytoplankton in a changing world: cell size and elemental stoichiometry. *Journal of Plankton Research*, 32, 119–137.
- Glibert, M. G., Wilkerson, F. P., Dugdale, R. C., Raven, J. A., Dupont, C. L., Leavitt, P. R., Parker, A. E., Burkholder, J. M., & Kana, T. M. (2016). Pluses and minuses of ammonium and nitrate uptake and assimilation by phytoplankton and implications for productivity and community composition, with emphasis on nitrogen-enriched conditions. *Limnology and Oceanography*, 61, 165–197.
- Guinder, V. A., Molinero, J. C., Popovich, C. A., Marcovecchio, J. E., & Sommer, U. (2012). Dominance of the planktonic diatom *Thalassiosira minima* in recent summers in the Bahia Blanca Estuary, Argentina. *Journal of Plankton Research*, 34, 995–1000.
- Hoppenrath, M., Beszteri, B., Drebes, G. et al. (2007). *Thalassiosira* species (Bacillariophyceae, Thalassiosirales) in the North Sea at Helgoland (German Bight) and Sylt (North Frisian Wadden Sea)-a first approach to assessing diversity. *European Journal of Phycology*, 42, 271–288.
- Horner, R. (2002) A taxonomic guide to some common phytoplankton. Dorchester, UK: Biopress Limited. Dorset Press.
- Khokhar, F. N, Naz, T., Burhan, Z. N., Abassi, M. J., & Siddiqui, P. J. A. (2018). Occurrence of HAB / toxic dinoflagellates species from the coast of Karachi, Pakistan (Northern Arabian Sea). *Indian Journal of Geo-Marine Sciences*, 47, 73-88.
- Lomas, M. W., & Glibert, P. M. (1999a). Interactions between NH_4^+ and NO_3^- uptake and assimilation: comparison of diatoms and dinoflagellates at several growth temperatures. *Marine Biology*, 133, 541-551.
- Lomas, M. W., & Glibert, P. M. (1999b). Temperature regulation of nitrate uptake: a novel hypothesis about nitrate uptake and reduction in cool water diatoms. *Limnology and Oceanography*, 44, 556-572.
- Margalef, R. (1978). Life forms of phytoplankton as survival alternatives in an unstable environment. *Oceanology Acta*, 1, 493-509.
- McQuoid, M. (2005) Influence of salinity on seasonal germination of resting stages and composition of microplankton on the Swedish west coast. *Marine Ecology Progress Series*, 289, 151–163.
- Menden-Deuer, S., & Lessard, E. J. (2000). Carbon to volume relationships from dinoflagellates, diatoms, and other protist plankton. *Limnology and Oceanography*, 45, 569-579.
- Mitbavkar, S., Rajaneesh, K., Anil, A., & Sundar, D. (2012). Picophytoplankton community in a tropical estuary: detection of *Prochlorococcus*-like populations. *Estuarine, Coastal and Shelf Science*, 107, 159–164.
- Moestrup, Ø., Akselmann, R., Fraga, S., Hoppenrath, M., Iwataki, M., Komárek, J., et al. (Eds) (2018). IOC-UNESCO taxonomic reference list of harmful micro algae. Accessed at <http://www.marinespecies.org/hab> on 2018-06-27.

- Mozetic, P., Cangini, M., France, J., Bastianini, M., Aubry, F. B., Buzancic, M., et al. (2019). Phytoplankton diversity in Adriatic ports: Lessons from the port baseline survey for the management of harmful algal species. *Marine Pollution Bulletin*, *147*, 117-132.
- Moore, E. R., Bullington, B. S., Weisberg, A. J., Jiang, Y., Chang, J., & Halsey, K. H. (2017). Morphological and transcriptomic evidence for ammonium induction of sexual reproduction in *Thalassiosira pseudonana* and other centric diatoms. *PLOS ONE*, *12*, e0181098.
- Oshima, Y., Hasegawa, M., Yasumoto, T., Hallegraeff, G. M., & Blackburn, S. (1987). Dinoflagellate *Gymnodinium catenatum* as the source of paralytic shellfish toxins in Tasmanian shellfish. *Toxicon*, *25*, 1105-1111.
- Padmakumar, K. B., Menon, N. R., & Sanjeevan, V. N. (2012). Is occurrence of harmful algal blooms in the exclusive economic zone of India on the rise? *International Journal of Oceanography*, <https://doi.org/10.1155/2012/263946>.
- Patgaonkar, R. S., Vethamony, P., Lokesh, K. S., & Babu, M. T. (2012). Residence time of pollutants discharged in the Gulf of Kachchh, northwestern Arabian Sea. *Marine Pollution Bulletin*, *64*, 1659-1666.
- Parsons, T. R., Maita, Y., & Lalli, C. M. (1984). A manual of biological and chemical methods for seawater analysis Oxford: Publ. Pergamon Press.
- Patil, J.S., & Anil, A. C. (2011). Variations in phytoplankton community in a monsoon influenced tropical estuary. *Environmental Monitoring and Assessment*, *182*, 291-300.
- Patil, J. S., & Anil, A. C. (2008). Temporal variation of diatom benthic propagules in a monsoon-influenced tropical estuary. *Continental Shelf Research*, *28*, 2404-2416.
- Qu, P., Fu, F., & Hutchins, D. A. (2018). Responses of the large centric diatom *Coscinodiscus* sp. to interactions between warming, elevated CO₂ and nitrate availability. *Limnology and Oceanography*, *61*, 1407-1424.
- Ramamurthy, S., & Dhawan, R. M. (1967). On the characteristics of the plankton at Kandla in the Gulf of Kutch. *Indian Journal of Fisheries*, *10*, 94-101.
- Rath, A. R., Mitbavkar, S., & Anil, A. C. (2018). Phytoplankton community structure in relation to environmental factors from the New Mangalore Port waters along the southwest coast of India. *Environmental monitoring and assessment*, *190*, 481-504.
- Rath, A. R., Mitbavkar, S., & Anil, A. C. (2021). Response of the phytoplankton community to seasonal and spatial environmental conditions in the Haldia port ecosystem located in the tropical Hooghly River estuary. *Environmental monitoring and assessment*, *193*, 548.
- Rodriguez-Ramos, T., Dornelas, M., Maranon, E., & Cermeno, P. (2014). Conventional sampling methods severely underestimate phytoplankton species richness. *Journal of Plankton Research*, *36*, 334-343.
- Roshith, C. M., Meena, D. K., Manna, R. K., Sahoo, A. K., Swain, H. S., Raman, R. K., Sengupta, A., & Das, B. K. (2018). Phytoplankton community structure of the Gangetic (Hooghly-Matla) estuary: Status and ecological implications in relation to eco-climatic variability. *Flora*, *240*, 133-143.

- Sanilkumar, M. G., Thomas, A. M., Shyamkumar, S., Philip, R., Mohammed Hatha, A. A., Sanjeevan, V. N., & Saramma, A. V. (2009). First report of *Protoperdinium* bloom from Indian waters. *Harmful Algae News*, 39, 15.
- Saravanae, N., Sachithanandam, V., Muruganandam, M., Nagaarjunan, P., & Mohan, P. M. (2016). Climatic change and anthropogenic influences on *Rhizosolenia imbricata* Brightwell 1858 Bacillariophyceae bloom in Sisostri Bay, Port Blair, Andaman, India. *Indian Journal of Geo-Marine Sciences*, 45, 425–430.
- Shirodkar, P. V., Pradhan, U. K., Fernandes, D., Haldankar, S. R., & Rao, G. S. (2010). Influence of anthropogenic activities on the existing environmental conditions of Kandla Creek (Gulf of Kutch). *Current Science*, 98, 815-828.
- Sin, Y., Hyun, B., Jeong, B., & Soh, H. Y. (2013). Impacts of eutrophic freshwater inputs on water quality and phytoplankton size structure in a temperate estuary altered by a sea dike. *Marine Environmental Research*, 85, 54–63.
- Sinha, P. C., Jena, G. K., Rao, A. D., & Jain, I. (2006). Numerical modelling of suspended sediment transport in the Gulf of Kachchh including Kandla creek, West Coast of India. *Marine Geodesy*, 29, 49–63.
- Smayda, T. J., & Reynolds, C. S. (2001). Community assembly in marine phytoplankton: application of recent models to harmful dinoflagellate blooms. *Journal of Plankton Research*, 23, 447–461.
- Snoeijs, P., Busse, S., & Potapova M. (2002). The importance of diatom cell size in community analysis. *Journal of Phycology*, 38, 265-272.
- Soler-Figueroa, B. M., Fontaine, D. N., Carney, K. J., Ruiz, G. M., & Tamburri, M. N. (2020). Characteristics of global port phytoplankton and implications for current ballast water regulations. *Marine Pollution Bulletin*, 155, 111165.
- Sournia, A. (1982). Form and function in marine phytoplankton. *Biological Reviews*, 57, 347-394.
- Spilling, K., Kremp, A., Klais, R., Olli, K., & Tamminen, T. (2014). Spring bloom community change modifies carbon pathways and C:N:P:Chl a stoichiometry of coastal material fluxes. *Biogeosciences*, 11, 7275–7289.
- Subrahmanyam, R. (1946). A systematic account of the marine plankton diatoms of the Madras coast, *Proceedings of the Indian Academy of Sciences-section B*, Springer, 85–197.
- ter Braak, C. J. F., & Smilauer, P. (2002). CANOCO reference manual and CanoDraw for Windows user's guide: software for canonical community ordination (version 4.5). Wageningen: TNO Institute of Applied Computer Science.
- Tomas, C. R. (1997). Identifying marine phytoplankton. Academic press.
- Thangaraja, M., Al-Aisry, A., & Al-Kharusi, L. (2007). Harmful algal blooms and their impacts in the middle and outer ROPME sea area. *International Journal of Oceans and Oceanography*, 2, 85-98.

- Thomas, L. C., Bijoy, N. S., & Padmakumar, K. B. (2020). Winter monsoon phytoplankton community in the coastal waters of Northeastern Arabian Sea, with emphasis on harmful and non-indigenous species. *Indian Journal of Geo-Marine Sciences*, 49, 989-999.
- Vijayalakshmy, K. C., Abhijith, M., Megha, M. K., Mohamed Hatha, A. A., & Saramma, A. V. (2019). Occurrence of algal bloom dominated by *Fragilariopsis oceanica* from the coastal waters of southwest India, off-Kannur. *Indian Journal of Geo Marine Sciences*, 48, 169-172.
- Vila, M., & Masó, M. (2005). Phytoplankton functional groups and harmful algae species in anthropogenically impacted waters of the NW Mediterranean Sea. *Scientia Marina*, 69, 31–45.
- Vollenweider, R., Giovanardi, F., Montanari, G., & Rinaldi, A. (1998). Characterization of the trophic conditions of marine coastal waters, with special reference to the NW Adriatic Sea: proposal for a trophic scale, turbidity and generalized water quality index. *Environmetrics*, 9, 329–357.
- Worden, A. Z., Nolan, J. K., & Palenik, B. (2004). Assessing the dynamics and ecology of marine picophytoplankton: The importance of the eukaryotic component. *Limnology and Oceanography*, 49, 168–179.

Figure legends

Fig. 1. Locations of sampling stations in the Kandla Port Trust ecosystem, west coast of India. (1) IOC jetty, (2) IFFCO jetty, (3) Fertilizer berth, (4-6) Oil jetties, (7-8) Local fishing craft anchorage, (9) Maintenance jetty, (10) Tug jetty, (11-20) Cargo berths, (21-26) Mangrove area

Fig. 2. Box-and-whisker plots of the environmental variables during PoM-I, MON, PoM-II and PrM in the surface and near bottom waters of the Industrial, major Activity and Mangrove areas of the Kandla Port Trust ecosystem. Temperature (a, b); salinity (c, d); DO (e, f); BOD (g, h); chlorophyll *a* (i, j); NO₃⁻ (k, l); NO₂⁻ (m, n); NH₄⁺ (o, p); PO₄³⁻ (q, r) and SiO₄⁴⁻ (s, t). In each plot, the median value is displayed with the small box, the big box limits represent the 25th (bottom) and 75th (top) percentiles, and the whiskers indicate the minimum and maximum values.

Fig. 3a. Relative contribution of the nano-microphytoplankton species representing > 1% of the total nano-microphytoplankton abundance during PoM-I, MON, PoM-II and PrM in the surface and near bottom waters of the Industrial area, major Activity area and Mangrove area of the Kandla Port Trust ecosystem. Size of the filled circles denote range of the relative contribution (%).

Fig. 3b. Relative contribution of the nano-microphytoplankton species representing < 1% of the total nano-microphytoplankton abundance during PoM-I, MON, PoM-II and PrM in the surface and near bottom waters of the Industrial area, major Activity area and Mangrove area of the Kandla Port Trust ecosystem. Size of the filled circles denote range of the relative contribution (%).

Fig. 4. Box-and-whisker plots of the cell abundance of Picophytoplankton (a, b); Nano-microphytoplankton (c, d); Diatoms (e, f); Centric diatoms (g, h); Pennate diatoms (i, j); Dinoflagellates (k, l); Phototrophic dinoflagellates (m, n); Heterotrophic dinoflagellates (o, p); Mixotrophic dinoflagellates (q, r) and Silicoflagellates (s, t) during PoM-I, MON, PoM-II and PrM in the surface and near bottom waters of the Industrial area, major Activity area and Mangrove area of the Kandla Port Trust ecosystem. In each plot, the median value is displayed with the small box, the big box limits represent the 25th (bottom) and 75th (top) percentiles, and the whiskers indicate the minimum and maximum values.

Fig. 5. Box-and-whisker plots of the carbon biomass of Picophytoplankton (a, b); Nano-microphytoplankton (c, d); Diatoms (e, f); Centric diatoms (g, h); Pennate diatoms (i, j); Dinoflagellates (k, l); Phototrophic dinoflagellates (m, n); Heterotrophic dinoflagellates (o, p); Mixotrophic dinoflagellates (q, r) and Silicoflagellates (s, t) during PoM-I, MON, PoM-II and PrM in the surface and near bottom waters of the Industrial area, major Activity area and Mangrove area of the Kandla Port Trust ecosystem. In each plot, the median value is displayed with the small box, the

big box limits represent the 25th (bottom) and 75th (top) percentiles, and the whiskers indicate the minimum and maximum values.

Fig. 6. Relative contribution (%) of the (a, d) nano-microphytoplankton groups (Bacillariophyceae, Dinophyceae, and Dictyophyceae) to the total NMP abundance (NMPA); (b, e) NMPA and picophytoplankton abundance to the total phytoplankton abundance (TPA) and (c, f) NMP and picophytoplankton carbon biomass to the total phytoplankton biomass (TPB) during PoM-I, MON, PoM-II and PrM in the surface and near bottom waters of the Industrial area, major Activity area and Mangrove area of the Kandla Port Trust ecosystem. Size of the filled circles denote range of the relative contribution (%).

Fig. 7. Redundancy Analysis biplot between the environmental variables (temperature, salinity, DO, BOD, NO₃⁻, NO₂⁻, NH₄⁺, PO₄³⁻, SiO₄⁴⁻, and TRIX) and phytoplankton groups in the Industrial (a), major Activity (b) and Mangrove (c) areas of the Kandla Port Trust ecosystem. Red dotted arrows indicate significant environmental variables.

Fig. 8. Redundancy Analysis biplot between the environmental variables (temperature, salinity, DO, BOD, NO₃⁻, NO₂⁻, NH₄⁺, PO₄³⁻, SiO₄⁴⁻, and TRIX) and nano-microphytoplankton species and sampling stations in the Industrial (a, b), major Activity (c, d) and Mangrove (e, f) areas of the Kandla Port Trust ecosystem. Red dotted arrows indicate significant environmental variables.

Supplementary Fig. 1. Distribution of the environmental variables in the surface and near bottom waters during PoM-I, MON, PoM-II and PrM in the surface and near bottom waters of the Industrial, major Activity and Mangrove areas of the Kandla Port Trust ecosystem.

Supplementary Fig. 2. The Bray-Curtis group average link cluster analysis for (a) surface and (b) near bottom nano-microphytoplankton community in the different zones (Industrial-Z1; major Activity-Z2; Mangrove-Z3) during the sampled seasons.

Table 1. Sampling details during the post-monsoon, monsoon and pre-monsoon seasons at the Kandla port (WD: Water depth; ETH: Estimated tidal height ; RF: Rainfall)

St. No.	Latitude (N)	Longitude (E)	Post-monsoon I (Oct 2014)			Monsoon (July 2015)			Post-monsoon II (Oct-Nov-2015)			Pre-monsoon (Feb-2016)										
			Date (d-m-y)	Time (h)	WD (m)	ETH (m)	RF (mm)	Date (d-m-y)	Time (h)	WD (m)	ETH (m)	RF (mm)	Date (d-m-y)	Time (h)	WD (m)	ETH (m)	RF (mm)					
1	23°02'31.3"	70°13'20.0"	14.10.14	07:30	09.0	05.73	00.0	29.07.15	08:30	08.5	02.11	33.5	31.10.15	08:40	08.4	04.01	00.0	06.02.16	08:08	08.4	02.39	00.0
2	23°02'17.0"	70°13'20.8"	14.10.14	07:05	11.5	06.03	00.0	29.07.15	08:00	11.0	01.64	33.5	31.10.15	09:00	11.8	03.71	00.0	06.02.16	07:48	11.8	02.17	00.0
3	23°02'04.1"	70°13'24.3"	14.10.14	06:37	11.5	03.36	00.0	29.07.15	07:30	11.0	01.16	33.5	01.11.15	08:15	11.8	05.04	00.0	06.02.16	07:10	11.8	02.16	00.0
4	23°01'54.4"	70°13'22.9"	14.10.14	05:50	12.2	06.00	00.0	29.07.15	07:15	12.0	00.93	33.5	01.11.15	08:30	12.5	04.83	00.0	06.02.16	06:50	12.5	02.39	00.0
5	23°02'12.6"	70°13'23.0"	15.10.14	07:15	11.3	06.15	00.0	30.07.15	08:50	11.0	01.43	34.8	31.10.15	06:45	11.6	05.73	00.0	06.02.16	06:25	11.6	02.67	00.0
6	23°02'00.9"	70°13'23.2"	15.10.14	06:47	13.2	05.97	00.0	30.07.15	08:25	13.0	00.99	34.8	31.10.15	07:05	13.5	05.43	00.0	06.02.16	06:05	13.5	02.90	00.0
7	23°01'16.3"	70°13'20.5"	13.10.14	09:12	07.8	03.98	00.0	27.07.15	07:55	07.0	02.36	09.8	30.10.15	09:15	07.8	02.68	00.0	05.02.16	07:45	07.8	02.91	00.0
8	23°01'03.0"	70°13'19.0"	13.10.14	08:45	07.8	04.35	00.0	27.07.15	08:10	07.0	03.58	09.8	30.10.15	08:35	07.8	03.30	00.0	05.02.16	07:30	07.8	02.77	00.0
9	23°00'45.1"	70°13'21.6"	16.10.14	06:00	07.9	04.62	00.0	31.07.15	06:00	07.0	02.67	34.8	02.11.15	06:00	08.2	05.92	00.0	05.02.16	07:15	08.2	02.63	00.0
10	23°00'26.0"	70°13'24.6"	13.10.14	07:54	11.6	05.03	00.0	27.07.15	08:30	11.0	03.83	09.8	30.10.15	08:10	11.4	04.46	00.0	08.02.16	06:00	11.4	03.89	00.0
11	23°00'19.7"	70°13'25.7"	13.10.14	07:32	12.4	05.33	00.0	27.07.15	07:30	12.0	03.09	09.8	30.10.15	07:40	12.2	04.16	00.0	05.02.16	07:00	12.2	02.50	00.0
12	23°00'13.3"	70°13'26.4"	13.10.14	07:16	11.5	05.54	00.0	27.07.15	07:15	11.0	02.91	09.8	30.10.15	07:15	11.4	04.55	00.0	05.02.16	06:45	11.4	02.36	00.0
13	23°00'01.8"	70°13'26.0"	13.10.14	06:50	14.0	05.89	00.0	27.07.15	07:00	14.0	02.72	09.8	30.10.15	07:00	14.5	04.79	00.0	05.02.16	06:30	14.5	02.24	00.0
14	22°59'44.7"	70°13'27.1"	13.10.14	06:06	18.2	06.48	00.0	27.07.15	06:30	18.0	02.36	09.8	30.10.15	06:15	18.2	05.49	00.0	05.02.16	06:10	18.2	02.44	00.0
15	22°59'32.0"	70°13'28.3"	12.10.14	08:45	15.4	03.75	00.0	26.07.15	08:45	15.0	04.01	08.0	29.10.15	08:30	15.8	02.56	00.0	04.02.16	08:15	15.8	03.86	00.0
16	22°59'29.8"	70°13'28.8"	12.10.14	09:05	14.2	03.45	00.0	26.07.15	08:15	14.0	03.64	08.0	29.10.15	08:10	14.6	02.88	00.0	04.02.16	08:00	14.6	03.74	00.0
17	22°59'23.7"	70°13'30.2"	12.10.14	09:20	15.3	03.24	00.0	26.07.15	07:50	15.0	03.34	08.0	29.10.15	07:45	16.0	03.28	00.0	04.02.16	07:45	16.0	03.62	00.0
18	22°59'17.3"	70°13'29.5"	12.10.14	08:10	16.6	04.26	00.0	26.07.15	07:30	16.0	03.09	08.0	29.10.15	07:20	16.0	03.68	00.0	04.02.16	07:20	16.0	03.41	00.0
19	22°59'02.4"	70°13'35.5"	12.10.14	07:40	16.4	04.69	00.0	26.07.15	07:24	16.0	03.82	08.0	29.10.15	06:55	16.0	04.08	00.0	04.02.16	07:00	16.0	03.25	00.0
20	22°58'53.3"	70°13'39.5"	12.10.14	06:11	20.2	05.99	00.0	26.07.15	06:40	20.0	02.48	08.0	29.10.15	06:10	20.4	04.80	00.0	04.02.16	06:40	20.4	03.08	00.0
21	22°58'56.7"	70°14'06.6"	15.10.14	08:47	06.0	05.19	00.0	30.07.15	06:45	05.0	01.32	34.8	01.11.15	06:30	06.5	06.49	00.0	07.02.16	07:15	06.5	02.47	00.0
22	22°59'32.5"	70°13'55.5"	15.10.14	08:30	06.2	05.37	00.0	30.07.15	07:05	04.5	01.04	34.8	01.11.15	06:45	06.4	06.28	00.0	07.02.16	07:00	06.4	02.65	00.0
23	23°0'53.2"	70°13'54.3"	15.10.14	08:08	05.8	05.60	00.0	30.07.15	07:35	04.8	00.61	34.8	01.11.15	07:05	06.2	06.01	00.0	07.02.16	06:48	06.2	02.08	00.0
24	23°02'10.2"	70°13'50.5"	15.10.14	07:43	06.2	05.86	00.0	30.07.15	08:00	05.3	00.54	34.8	01.11.15	07:25	06.8	05.73	00.0	07.02.16	06:30	06.8	03.03	00.0
25	23°2'33.8"	70°13'35.1"	14.10.14	08:15	05.8	05.19	00.0	29.07.15	09:30	04.6	03.06	33.5	31.10.15	07:30	06.5	05.05	00.0	07.02.16	06:10	06.5	03.28	00.0
26	23°02'52.0"	70°13'30.9"	14.10.14	07:50	06.0	05.49	00.0	29.07.15	08:45	04.6	02.35	33.5	31.10.15	08:10	06.2	04.46	00.0	06.02.16	08:25	06.2	02.58	00.0

Table 2. PERMANOVA results for the environmental variables and cell abundance of pico- and nano-microphytoplankton

Variables	Zone (Z)	Season (S)	Depth (D)	Z x S	Z x D	S x D	Z x S x D
Temp	0.059	0.001	0.973	0.023	1.000	1.000	1.000
Salinity	0.007	0.001	0.988	0.014	0.993	0.938	0.993
DO	0.002	0.001	0.499	0.001	0.923	0.865	1.000
BOD	0.473	0.018	0.060	0.001	0.207	0.282	0.965
NO ₃ ⁻	0.001	0.001	0.484	0.001	0.802	0.715	0.630
NO ₂ ⁻	0.652	0.001	0.750	0.420	0.852	0.652	0.897
NH ₄ ⁺	0.528	0.001	0.256	0.088	0.308	0.855	0.600
PO ₄ ³⁻	0.132	0.001	0.379	0.011	0.215	0.574	0.060
SiO ₄ ⁴⁻	0.401	0.001	0.437	0.430	0.267	0.363	0.500
Chl <i>a</i>	0.091	0.001	0.458	0.001	0.056	0.329	0.556
Cell abundance							
Centrics	0.307	0.057	0.167	0.019	0.748	0.489	0.939
Pennates	0.706	0.077	0.014	0.051	0.388	0.578	0.231
Phototrophic	0.186	0.012	0.071	0.833	0.547	0.017	0.712
Heterotrophic	0.373	0.378	0.381	0.370	0.356	0.387	0.374
Mixotrophic	0.647	0.911	0.610	0.590	0.694	0.549	0.554
Silicoflagellates	0.077	0.925	0.004	0.101	0.076	0.899	0.087
Diatoms	0.710	0.114	0.027	0.056	0.509	0.511	0.368
Dinoflagellates	0.144	0.031	0.085	0.818	0.579	0.031	0.525
NMP	0.734	0.123	0.021	0.039	0.479	0.506	0.360
Pico abundance	0.050	0.001	0.541	0.304	0.056	0.683	0.336
Carbon biomass							
NMP	0.791	0.256	0.244	0.389	0.689	0.633	0.413
Pico	0.665	0.100	0.481	0.979	0.635	0.541	0.724

Table 3. Nano-microphytoplankton species observed in the Kandla Port Trust during the monsoon, post-monsoon and pre-monsoon seasons

Phytoplankton groups	Species	Species codes	Seasons	Depth	IOC references	Other references
Diatoms (Centrics)	<i>Coscinodiscus radiatus</i> ^b	DC1	PoM I & II, MON, PrM	Sur & NBW		^b Rath et al., 2021
	<i>Coscinodiscus</i> sp.	DC2	PrM	Sur		
	<i>Ditylum brightwellii</i> ^b	DC3	PoM I,II, MON, PrM	Sur & NBW		^b D'Silva et al., 2012
	<i>Melosira nummuloides</i>	DC4	PoM I & II	Sur & NBW		
	<i>Odontella aurita</i>	DC5	PoM II, PrM	Sur & NBW		
	<i>Odontella mobiliensis</i>	DC6	PoM I & II, MON, PrM	Sur & NBW		
	<i>Odontella sinensis</i>	DC7	PoM I & II, MON	Sur & NBW		
	<i>Paralia sulcata</i>	DC8	PoM I & II, MON, PrM	Sur & NBW		
	<i>Planktoniella blanda</i>	DC9	PrM	Sur & NBW		
	<i>Rhizosolenia imbricata</i> ^b	DC10	PoM I & II, MON, PrM	Sur & NBW		^b Saravanae et al. 2016; Rath et al., 2018
(Pennates)	<i>Rhizosolenia setigera</i>	DC11	PoM I, PrM	Sur & NBW		
	<i>Thalassiosira</i> sp.1 ^b	DC12	PoM II, MON, PrM	Sur & NBW		^b D'Silva et al., 2012
	<i>Thalassiosira</i> sp.2	DC13	PoM I & II, MON, PrM	Sur & NBW		
	<i>Triceratium bicornes</i>	DC14	PoM II, PrM	Sur & NBW		
	<i>Triceratium favus</i> ^b	DC15	PoM II, MON, PrM	Sur & NBW		
	<i>Triceratium</i> sp.	DC16	PoM I & II, MON, PrM	Sur & NBW		
	<i>Amphiprora</i> sp.	DP1	PoM II, PrM	Sur & NBW		
	<i>Campylodiscus brightwellii</i>	DP2	MON	NBW		
	<i>Cocconeis</i> sp.	DP3	PoM II, MON, PrM	Sur & NBW		
	<i>Diploneis</i> sp.	DP4	PoM I & II, MON, PrM	Sur & NBW		
	<i>Fragilariopsis</i> sp. ^b	DP5	PoM I & II, MON, PrM	Sur & NBW		^b Vijayalakshmy et al., 2019
	<i>Gyrosigma balticum</i>	DP6	PoM I & II, MON, PrM	Sur & NBW		
	<i>Gyrosigma fasciola</i>	DP7	PoM I & II, PrM	Sur & NBW		
<i>Lauderia</i> sp.	DP8	PoM I, PrM	Sur & NBW			
<i>Navicula delicatula</i>	DP9	PoM I, PrM	Sur & NBW			
<i>Navicula derasa</i>	DP10	PoM I & II, PrM	Sur & NBW			
<i>Navicula</i> sp.1	DP11	PoM I & II, MON, PrM	Sur & NBW			
<i>Navicula</i> sp.2	DP12	PoM II, MON, PrM	Sur & NBW			
<i>Navicula</i> sp.3	DP13	PoM II, MON, PrM	Sur & NBW			

Table 3 (Continued)

Phytoplankton groups	Species	Species codes	Seasons	Depth	IOC references	Other references
	<i>Nitzschia</i> sp.1	DP14	PoM I & II, MON, PrM	Sur & NBW		
	<i>Nitzschia</i> sp.2	DP15	MON, PrM	Sur		
	<i>Nitzschia</i> sp.3	DP16	PoM II, PrM	Sur & NBW		
	<i>Nitzschia</i> sp.4	DP17	PrM	NBW		
	<i>Pleurosigma elongatum</i>	DP18	PoM I & II, MON, PrM	Sur & NBW		
	<i>Pleurosigma</i> sp.	DP19	PoM II, MON	Sur & NBW		
	<i>Pseudo-nitzschia</i> sp. ^a	DP20	PrM	Sur	Toxic	^a Moestrup et al. 2018
	<i>Surirella fastuosa</i>	DP21	PoM I & II, MON, PrM	Sur & NBW		
	<i>Tabellaria</i> sp.	DP22	PoM II, MON, PrM	Sur & NBW		
	<i>Thalassionema nitzschioides</i> ^b	DP23	PoM I & II, PrM	Sur & NBW		^b Vila and Maso 2005; Roshith et al., 2018
	<i>Thalassiothrix longissima</i> ^b	DP24	PoM I & II, MON, PrM	Sur & NBW		^b D'Silva et al., 2012
	<i>Trachyneis aspera</i>	DP25	MON, PrM	Sur & NBW		
Dinoflagellates (Phototrophic)	<i>Gymnodinium</i> sp. ^a	DFP1	PrM	Sur	Toxic	^a Anderson et al., 1989
	<i>Pyrophacus</i> sp.	DFP2	PoM II, MON, PrM	Sur & NBW		
Heterotrophic	<i>Protoperdinium</i> sp. ^b	DFH1	PoM I	Sur		^b Sanilkumar et al., 2009
Mixotrophic	<i>Tripos furca</i> ^b	DFM1	PoM I & II, PrM	Sur & NBW		^b Doan-Nhu and Nguyen-Ngoc 2017; Roshith et al., 2018
Silicoflagellates	<i>Dictyocha fibula</i> ^b	SF1	PoM I & II, MON, PrM	Sur		^b Vila and Maso 2005
	<i>Dictyocha octonaria</i>	SF2	PoM I	Sur		

^a Potential toxic species; ^b Potential harmful/bloom forming species; ^c First time reported in this area

Table 4. The dominant nano-microphytoplankton species observed in the surface and near bottom waters during the post monsoon, monsoon and pre-monsoon seasons. Bold values denote cell abundance ($\times 10^3$ cells L⁻¹)

Phytoplankton groups	Zones	PoM-I		MON		PoM-II		PrM	
		Surface	NBW	Surface	NBW	Surface	NBW	Surface	NBW
Diatoms (Centrics)	Industrial area	<i>Coscinodiscus radiatus</i> (11.4)	<i>Coscinodiscus radiatus</i> (3.4)	<i>Thalassiosira</i> sp. 2 (3.5)	<i>Thalassiosira</i> sp. 2 (6.1)	<i>Thalassiosira</i> sp. 2 (8.3)	<i>Paralia sulcata</i> (5.7)	<i>Thalassiosira</i> sp. 1 (7.0)	<i>Paralia Sulcata</i> (3.0)
	Major activity area	<i>Paralia sulcata</i> (5.8)	<i>Coscinodiscus radiatus</i> (3.4)	<i>Thalassiosira</i> sp. 2 (6.6)	<i>Thalassiosira</i> sp. 2 (9.1)	<i>Thalassiosira</i> sp. 2 (4.1)	<i>Paralia sulcata</i> (6.4)	<i>Thalassiosira</i> sp. 1 (9.6)	<i>Thalassiosira</i> sp. 1 (4.2)
	Mangrove area	<i>Coscinodiscus radiatus</i> (4.8)	<i>Odontella mobiliensis</i> (2.4)	<i>Thalassiosira</i> sp. 2 (5.5)	<i>Thalassiosira</i> sp. 2 (5.5)	<i>Paralia sulcata</i> (4.9)	<i>Paralia sulcata</i> (4.0)	<i>Thalassiosira</i> sp. 1 (3.9)	<i>Thalassiosira</i> sp. 1 (2.8)
(Pennates)	Industrial area	<i>Fragilariopsis</i> sp. (15.4)	<i>Thalassiothrix longissima</i> (3.9)	<i>Fragilariopsis</i> sp. (3.6)	<i>Fragilariopsis</i> sp. (5.5)	<i>Fragilariopsis</i> sp. (8.1)	<i>Fragilariopsis</i> sp. (13.9)	<i>Fragilariopsis</i> sp. (14.5)	<i>Thalassiothrix longissima</i> (6.1)
	Major activity area	<i>Fragilariopsis</i> sp. (8.3)	<i>Fragilariopsis</i> sp. (4.9)	<i>Nitzschia</i> sp. 1 (5.4)	<i>Nitzschia</i> sp. 1 (5.7)	<i>Fragilariopsis</i> sp. (11.3)	<i>Fragilariopsis</i> sp. (7.0)	<i>Thalassiothrix longissima</i> (6.8)	<i>Fragilariopsis</i> sp. (6.3)
	Mangrove area	<i>Fragilariopsis</i> sp. (10.4)	<i>Fragilariopsis</i> sp. (6.6)	<i>Nitzschia</i> sp. 1 (4.5)	<i>Nitzschia</i> sp. 1 (4.6)	<i>Fragilariopsis</i> sp. (8.0)	<i>Fragilariopsis</i> sp. (6.4)	<i>Thalassiothrix longissima</i> (4.9)	<i>Thalassiothrix longissima</i> (5.3)
Dinoflagellate	Industrial area	<i>Protoperidinium</i> sp. (0.1)		<i>Pyrophacus</i> sp. (0.1)		<i>Pyrophacus</i> sp. (0.1)	<i>Pyrophacus</i> sp. (0.1)	<i>Gymnodinium</i> sp. (0.1)	
	Major activity area	<i>Tripos Furca</i> (0.1)		<i>Pyrophacus</i> sp. (0.1)	<i>Pyrophacus</i> sp. (1.8)		<i>Tripos furca</i> (0.1)	<i>Pyrophacus</i> sp. (0.4)	<i>Tripos Furca</i> (0.1)
	Mangrove area			<i>Pyrophacus</i> sp. (0.1)			<i>Pyrophacus</i> sp. (0.1)		
Silicoflagellate	Industrial area	<i>Dictyocha octonaria</i> (0.1)					<i>Dictyocha fibula</i> (0.1)		
	Major activity area								
	Mangrove area			<i>Dictyocha fibula</i> (0.1)		<i>Dictyocha fibula</i> (0.1)			

Table 5. The Shannon-Wiener index of diversity (H'), Margalef's index of species richness (d), Pielou's index of evenness (J') and Trophic Index (TRIX) values during the sampled seasons in the surface and near bottom waters of the Kandla Port

	Post Monsoon-I						Monsoon					
	Surface			NBW			Surface			NBW		
	Industrial	Activity	Mangrove	Industrial	Activity	Mangrove	Industrial	Activity	Mangrove	Industrial	Activity	Mangrove
H'	1.71 ± 0.16	1.55 ± 0.20	1.30 ± 0.25	1.28 ± 0.27	1.27 ± 0.43	1.41 ± 0.28	1.59 ± 0.41	1.55 ± 0.26	1.52 ± 0.33	1.31 ± 0.57	1.72 ± 0.23	1.42 ± 0.22
d	0.94 ± 0.17	0.67 ± 0.21	0.58 ± 0.22	0.58 ± 0.25	0.55 ± 0.11	0.59 ± 0.16	0.76 ± 0.29	0.65 ± 0.22	0.64 ± 0.26	0.69 ± 0.12	0.85 ± 0.22	0.62 ± 0.15
j'	0.73 ± 0.04	0.79 ± 0.04	0.72 ± 0.07	0.83 ± 0.06	0.79 ± 0.08	0.76 ± 0.05	0.79 ± 0.12	0.81 ± 0.09	0.79 ± 0.03	0.75 ± 0.13	0.78 ± 0.06	0.75 ± 0.04
TRIX	3.6 ± 0.3	3.4 ± 0.3	3.4 ± 0.2	3.6 ± 0.3	3.4 ± 0.4	3.6 ± 0.3	3.2 ± 0.5	3.4 ± 0.2	3.6 ± 0.6	2.3 ± 0.7	2.4 ± 1.1	3.3 ± 0.9
	Post Monsoon-II						Pre Monsson					
	Surface			NBW			Surface			NBW		
	Industrial	Activity	Mangrove	Industrial	Activity	Mangrove	Industrial	Activity	Mangrove	Industrial	Activity	Mangrove
H'	1.80 ± 0.34	1.83 ± 0.18	1.82 ± 0.11	1.77 ± 0.21	1.75 ± 0.14	1.73 ± 0.19	2.01 ± 0.18	1.90 ± 0.21	2.07 ± 0.13	1.68 ± 0.18	1.89 ± 0.21	1.89 ± 0.27
d	1.01 ± 0.38	0.94 ± 0.25	0.90 ± 0.12	1.00 ± 0.13	0.93 ± 0.15	0.88 ± 0.23	1.35 ± 0.19	1.25 ± 0.18	1.26 ± 0.17	0.82 ± 0.23	1.06 ± 0.28	1.09 ± 0.41
j'	0.77 ± 0.08	0.80 ± 0.06	0.81 ± 0.07	0.75 ± 0.10	0.77 ± 0.06	0.78 ± 0.04	0.75 ± 0.05	0.73 ± 0.06	0.81 ± 0.06	0.79 ± 0.07	0.79 ± 0.03	0.80 ± 0.05
TRIX	3.5 ± 0.3	3.7 ± 0.4	3.5 ± 0.4	3.1 ± 0.4	3.6 ± 0.4	3.4 ± 0.4	4.1 ± 0.2	3.5 ± 0.5	3.1 ± 0.8	3.8 ± 0.3	3.5 ± 0.7	3.2 ± 0.4

Table 6. Marginal and conditional effects obtained from the summary of forward selection from the RDA for the nano-microphytoplankton (Bacillariophyceae and Dictyophyceae) and Picophytoplankton (Picocyanophytes + picoeukaryotes) and environmental variables. Lambda (I) refers to eigenvalues explained by the environmental variables. Bold values denote statistical significance ($p < 0.05$)

Marginal Effects		Conditional Effects		<i>p</i>
Variable	Lamb	Variable	Lambda (I)	
a) Industrial Area				
Temp		Temp		
Sal		SiO ₄ ⁴⁻		
NH ₄ ⁺		Sal		
DO		NH ₄ ⁺		
SiO ₄ ⁴⁻		NO ₃ ⁻		
TRIX		TRIX		
PO ₄ ³⁻		BOD		
BOD		PO ₄ ³⁻		
NO ₃ ⁻		NO ₂ ⁻		
NO ₂ ⁻		DO		
b) Major Activity Area				
NO ₃ ⁻		NO ₃ ⁻		
Temp		NO ₂ ⁻		
NH ₄ ⁺		SiO ₄ ⁴⁻		
SiO ₄ ⁴⁻		NH ₄ ⁺		
NO ₂ ⁻		TRIX		
PO ₄ ³⁻		BOD		
BOD		Temp		
Sal		DO		
DO		Sal		
TRIX		PO ₄ ³⁻		
c) Mangrove Area				
NO ₂ ⁻		NO ₂ ⁻		
Sal		SiO ₄ ⁴⁻		
SiO ₄ ⁴⁻		DO		
TRIX		Temp		
BOD		BOD		
NH ₄ ⁺		TRIX		
DO		NO ₃ ⁻		
PO ₄ ³⁻		NH ₄ ⁺		
NO ₃ ⁻		PO ₄ ³⁻		
Temp		Sal		

Table 7. Marginal and conditional effects obtained from the summary of forward selection from the RDA between the nano-microphytoplankton (Bacillariophyceae, Dinophyceae and Dictyophyceae) species and environmental variables of (a) Industrial (b) major Activity and (c) Mangrove areas. Lambda (I) refers to eigenvalues explained by the environmental variables. Bold values denote statistical significance ($p < 0.05$)

Marginal Effects		Conditional Effects		
Variable	Lambda (I)	Variable	Lambda (I)	<i>p-value</i>
a) Industrial Area				
NH ₄ ⁺	0.13	NH ₄ ⁺	0.13	0.001
SiO ₄ ⁴⁻	0.11	SiO ₄ ⁴⁻	0.1	0.001
Temp	0.08	PO ₄ ³⁻	0.04	0.001
PO ₄ ³⁻	0.06	Sal	0.03	0.002
Sal	0.06	Temp	0.02	0.026
NO ₃ ⁻	0.06	DO	0.02	0.177
NO ₂ ⁻	0.03	BOD	0.01	0.297
DO	0.02	NO ₂ ⁻	0.01	0.31
BOD	0.02	NO ₃ ⁻	0.01	0.637
b) Major Activity area				
NH ₄ ⁺	0.16	NH ₄ ⁺	0.16	0.001
Temp	0.13	SiO ₄ ⁴⁻	0.09	0.001
SiO ₄ ⁴⁻	0.11	Temp	0.03	0.001
Sal	0.06	Sal	0.02	0.012
NO ₃ ⁻	0.05	NO ₂ ⁻	0.01	0.084
DO	0.05	PO ₄ ³⁻	0.01	0.199
NO ₂ ⁻	0.03	NO ₃ ⁻	0.01	0.282
PO ₄ ³⁻	0.02	BOD	0.00	0.903
BOD	0.02	DO	0.01	0.811
c) Mangrove Area				
NH ₄ ⁺	0.18	NH ₄ ⁺	0.18	0.001
Temp	0.16	SiO ₄ ⁴⁻	0.09	0.001
SiO ₄ ⁴⁻	0.12	Temp	0.05	0.001
NO ₂ ⁻	0.09	NO ₂ ⁻	0.02	0.038
Sal	0.08	PO ₄ ³⁻	0.02	0.217
NO ₃ ⁻	0.06	Sal	0.02	0.468
PO ₄ ³⁻	0.05	DO	0.01	0.484
DO	0.03	BOD	0.01	0.565
BOD	0.02	NO ₃ ⁻	0.01	0.943

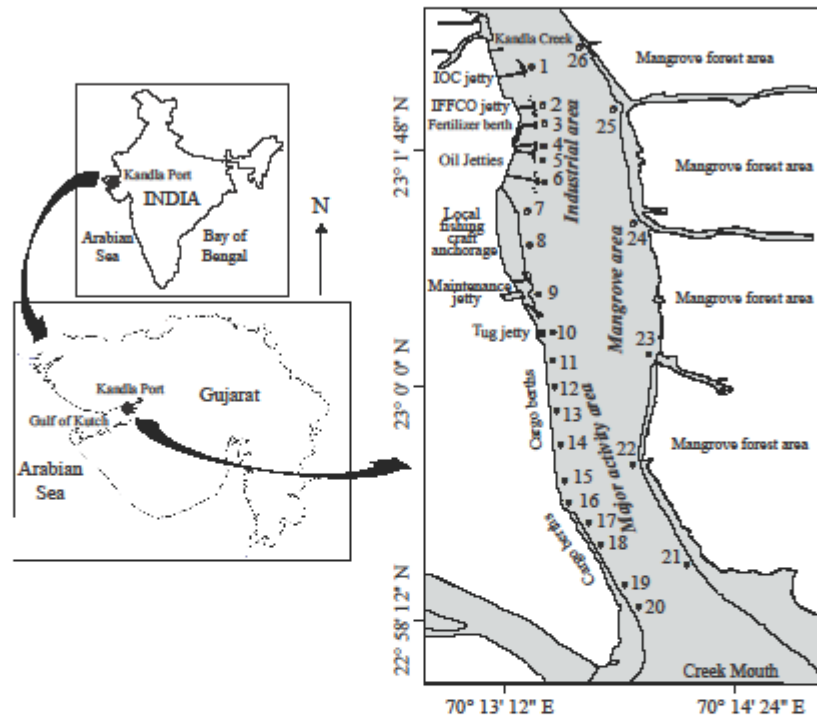


Fig. 1

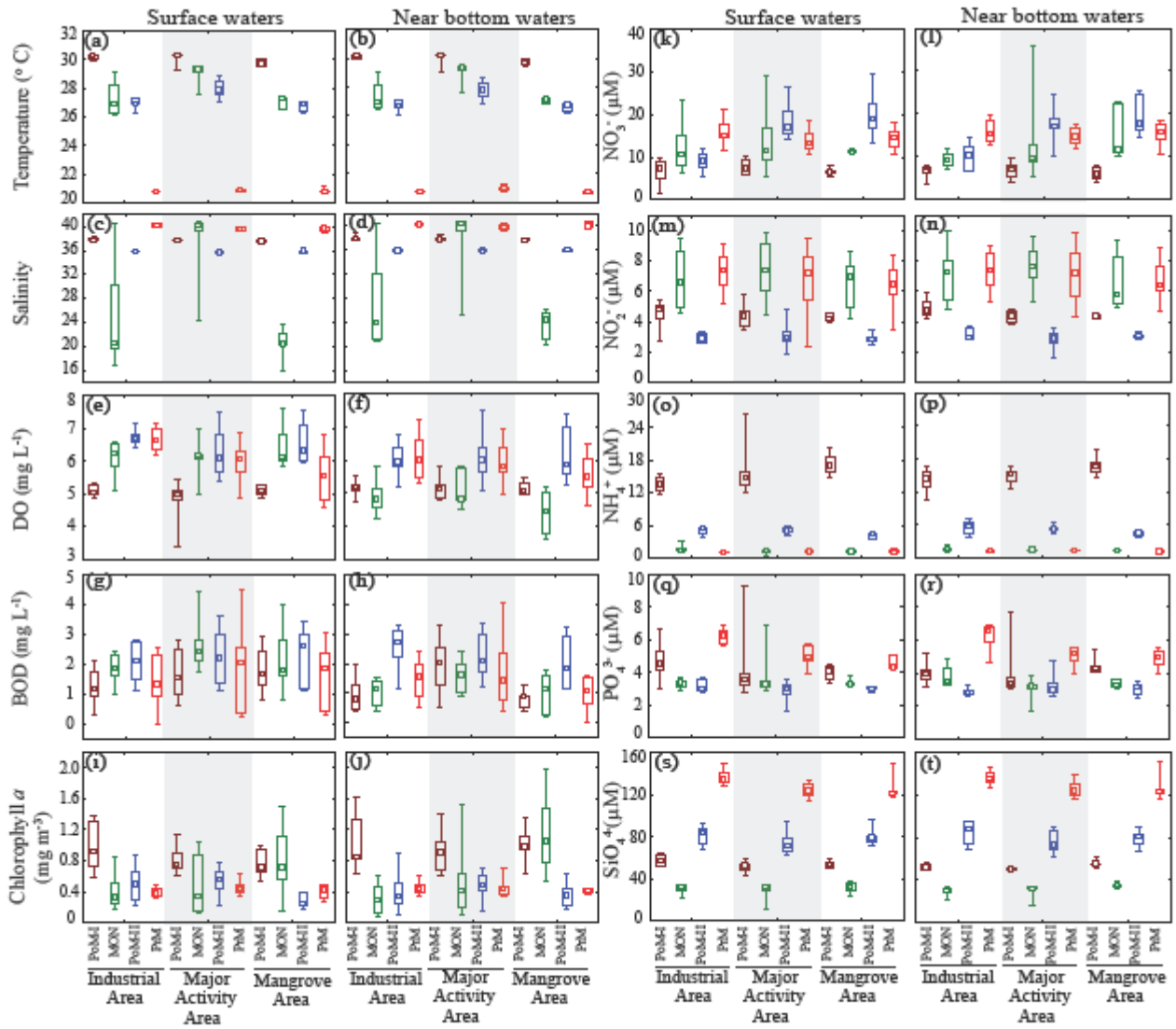


Fig. 2

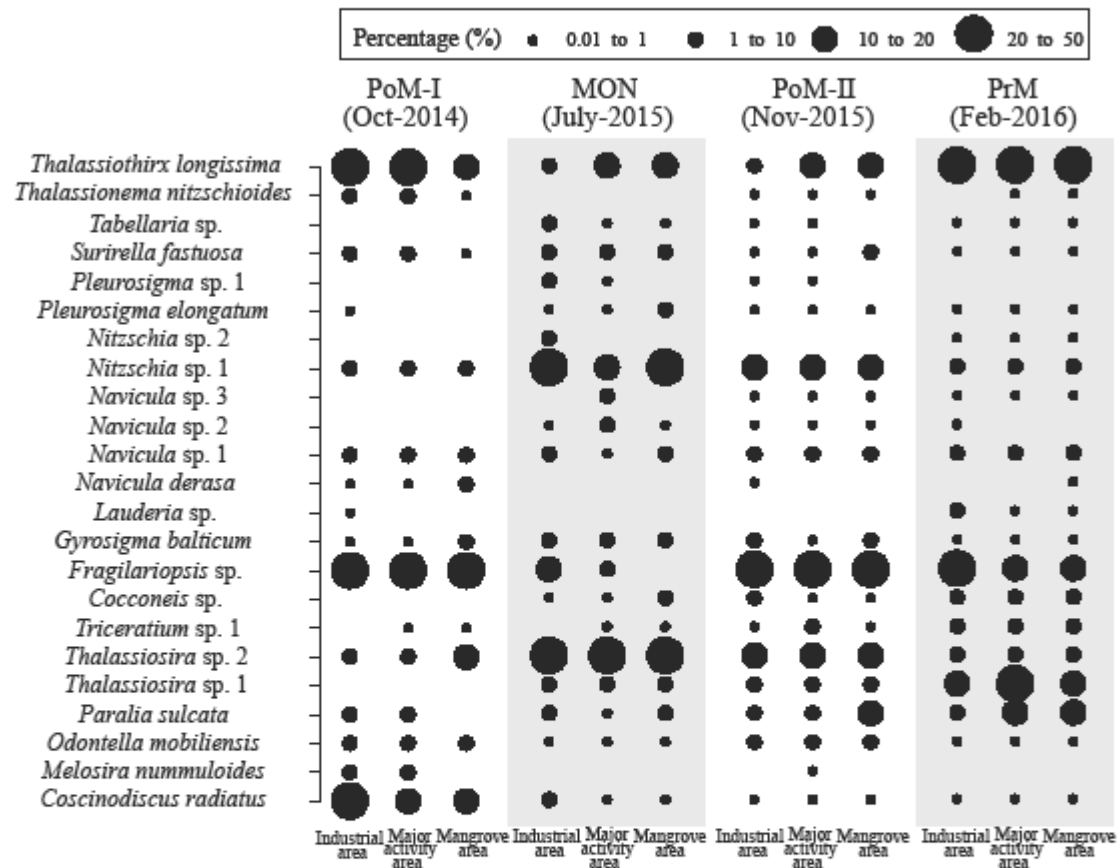


Fig. 3a

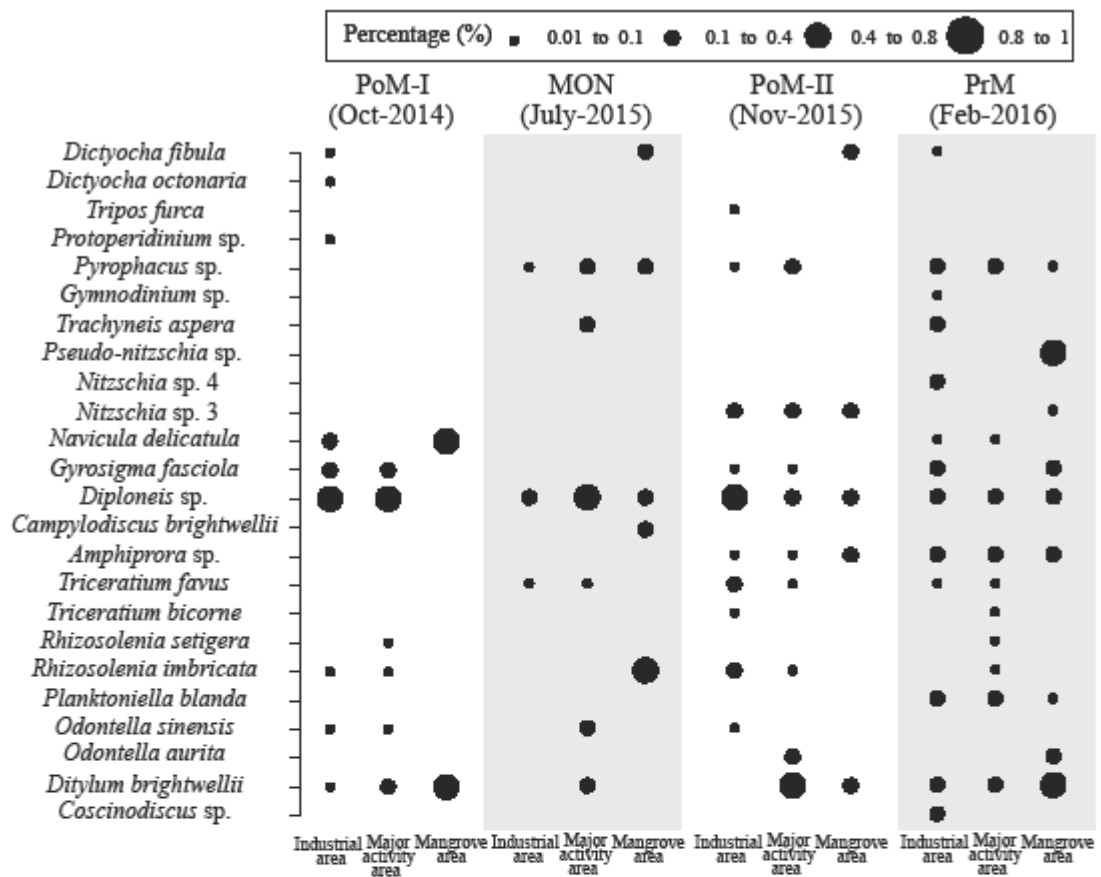


Fig. 3b

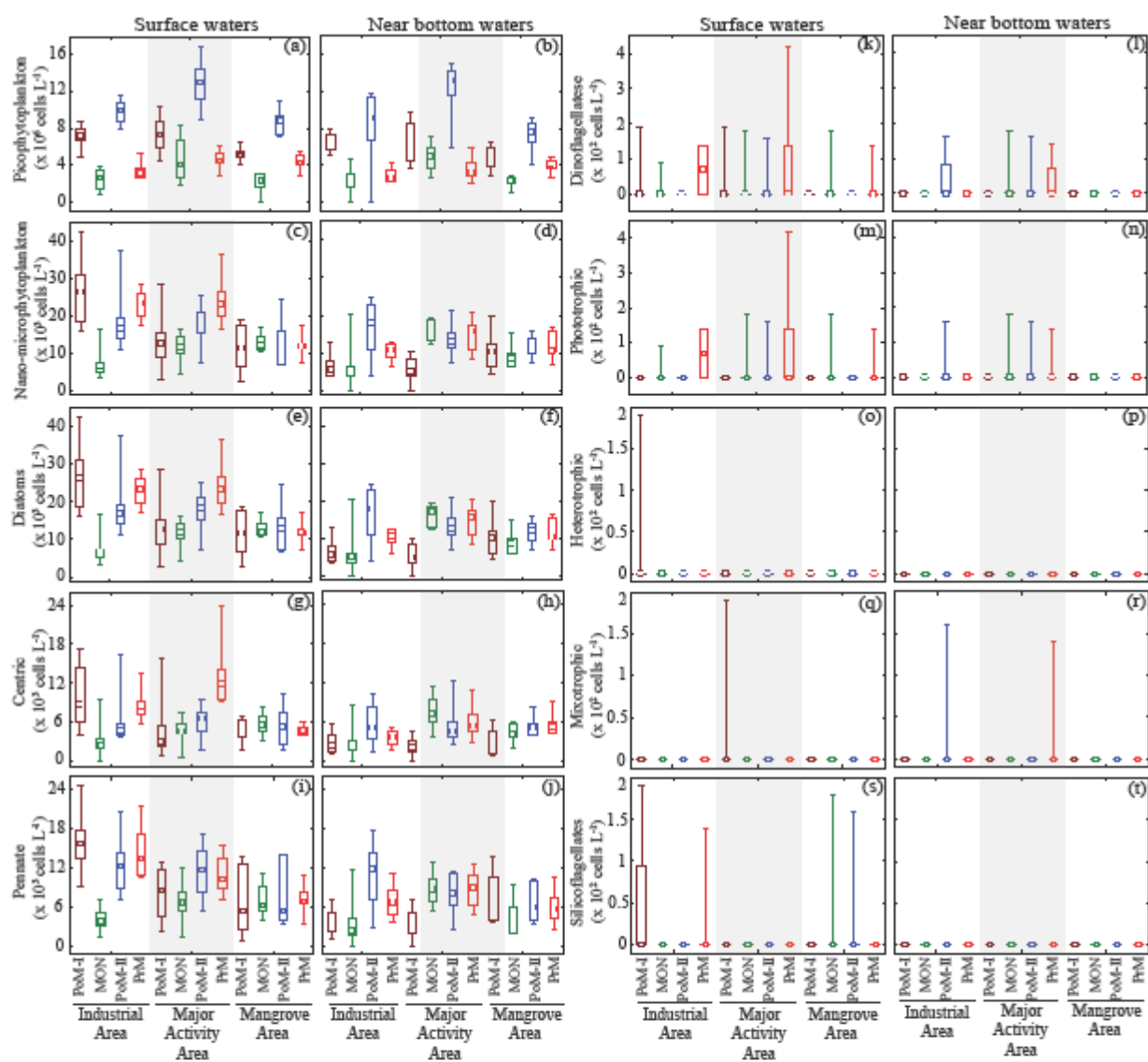


Fig. 4

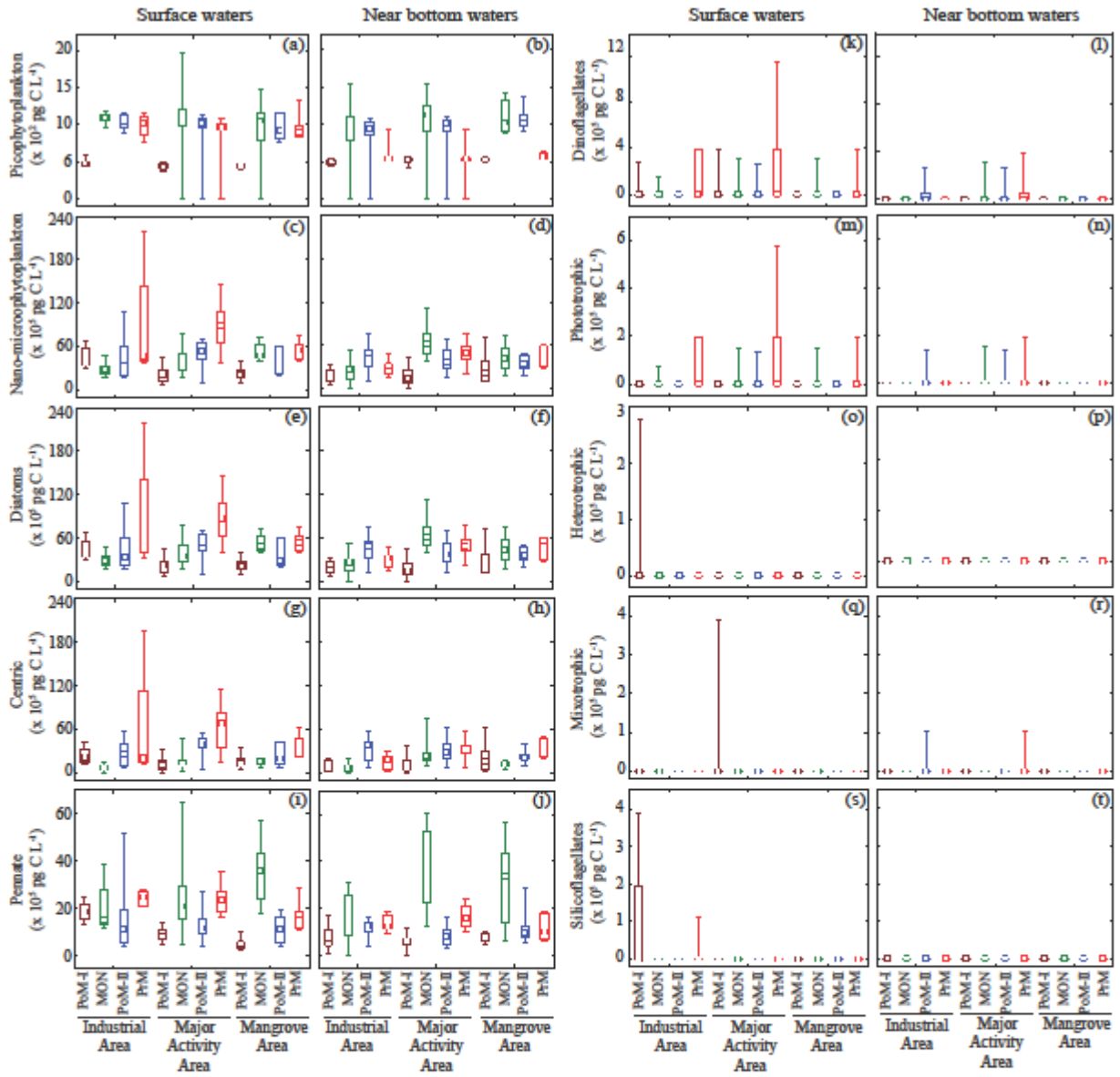


Fig. 5

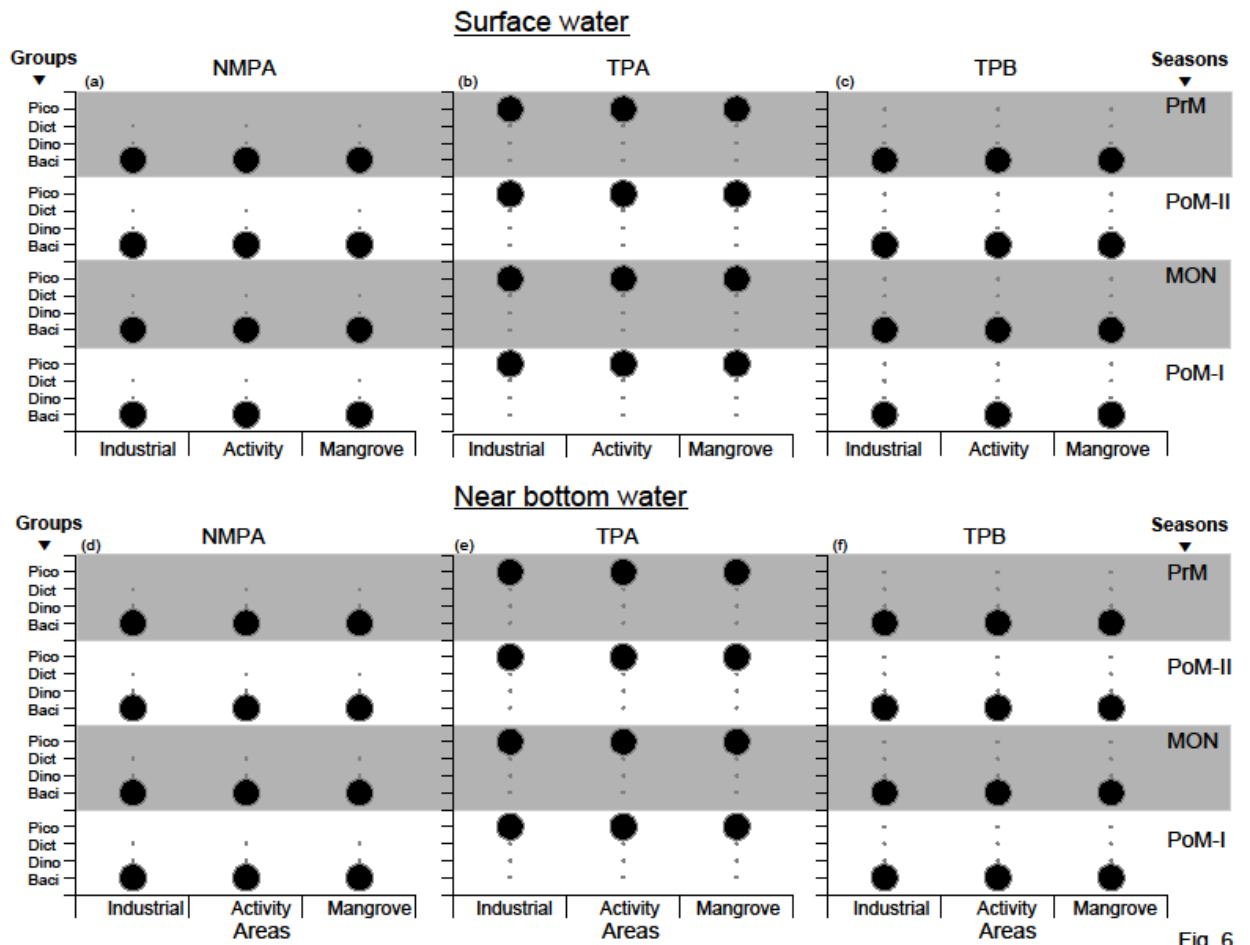


Fig. 6

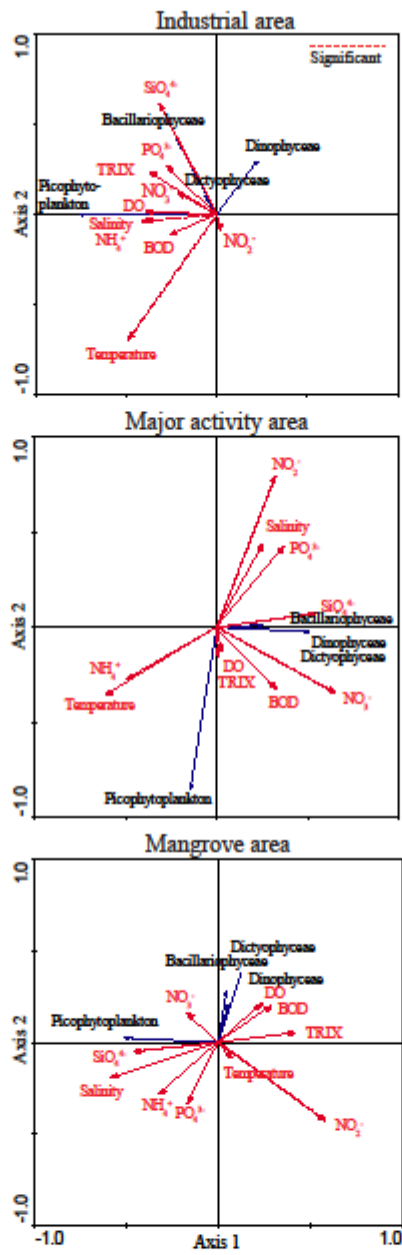


Fig. 7

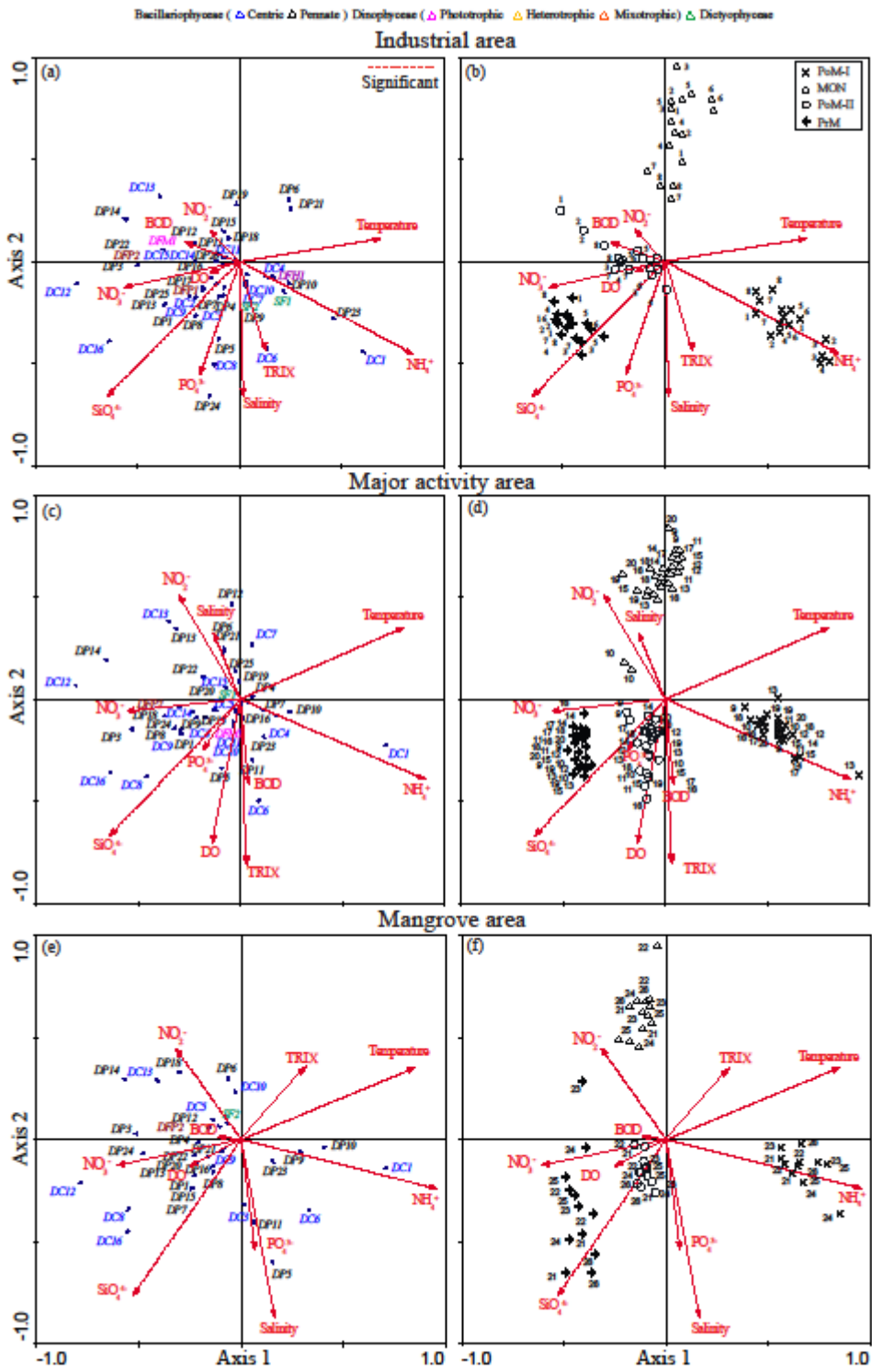
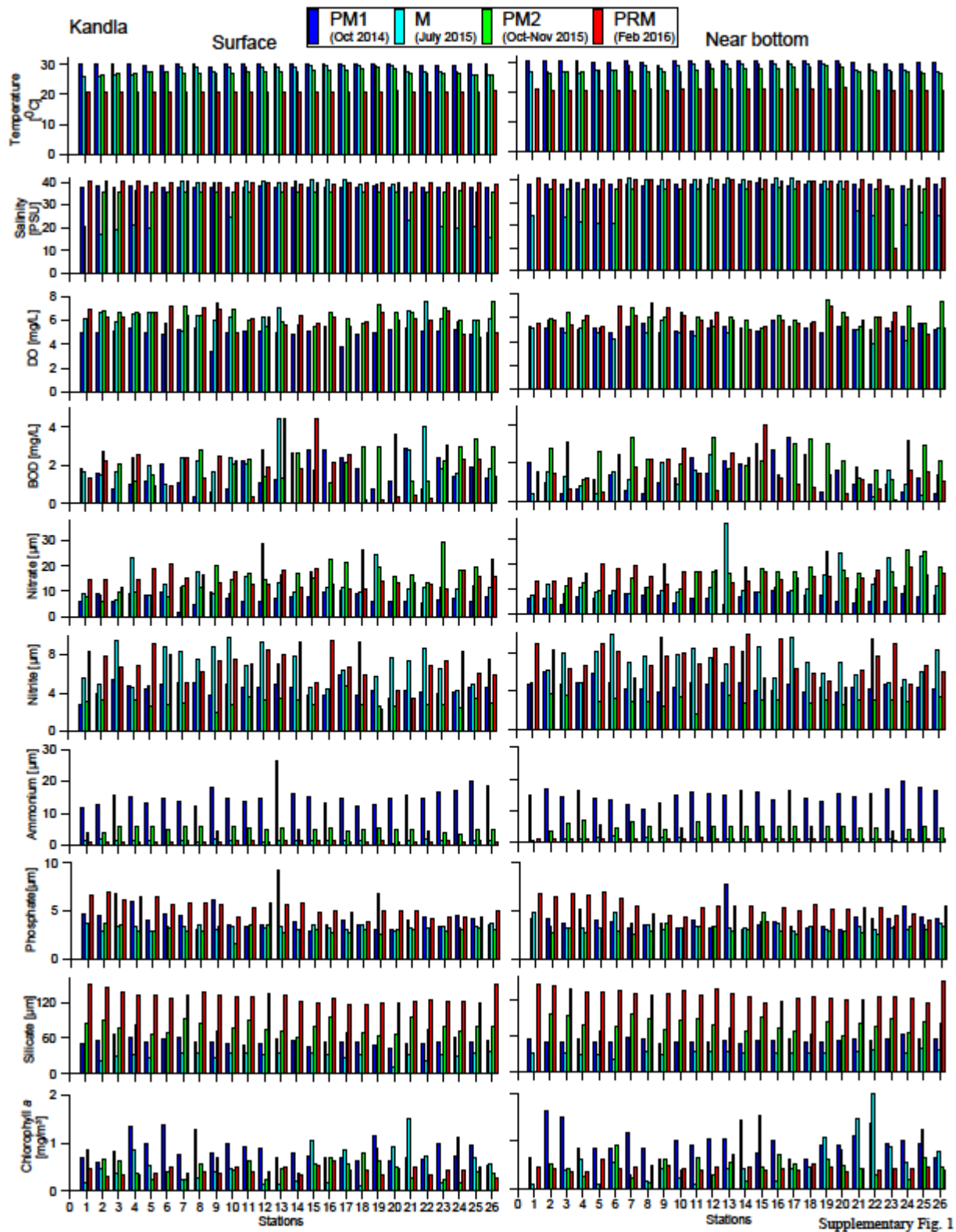
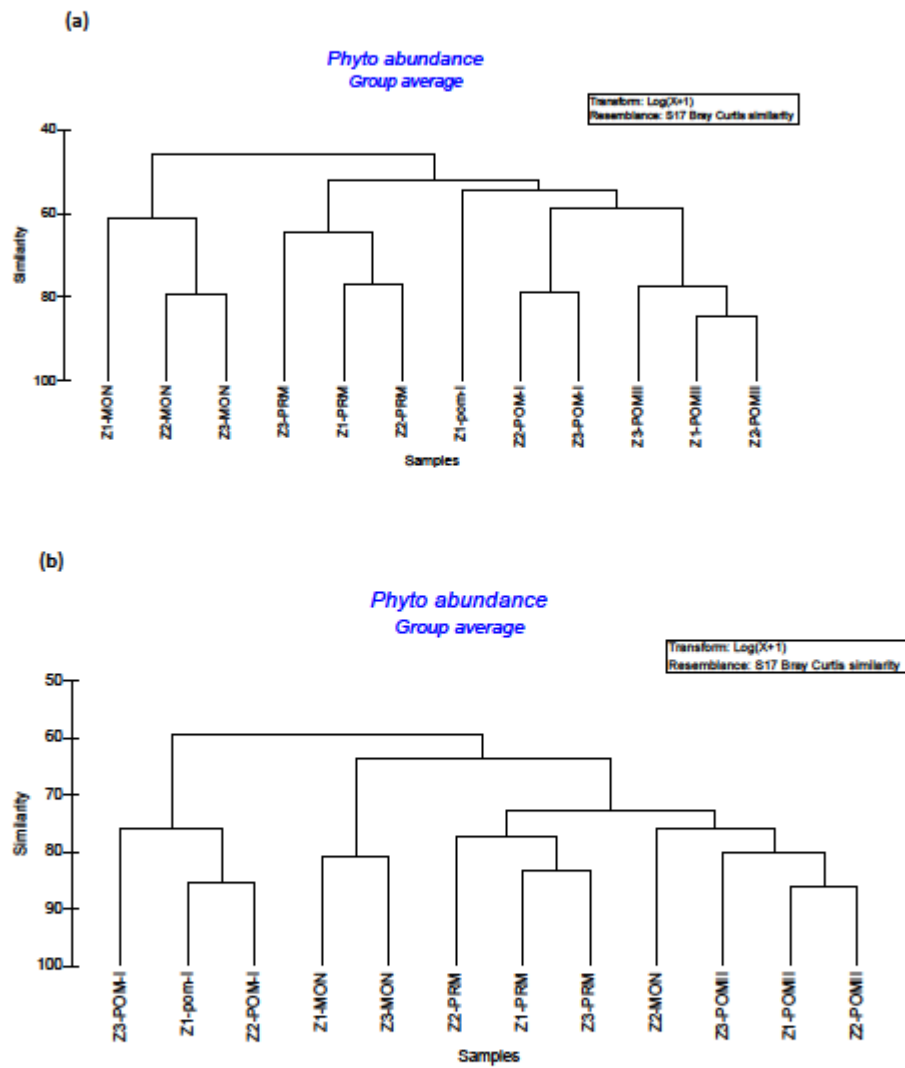


Fig. 8



Supplementary Fig. 1



Supplementary Fig. 2